

Georgia State University

ScholarWorks @ Georgia State University

Chemistry Theses

Department of Chemistry

Summer 8-10-2022

Synthesis and Characterization of Carbon Monoxide Prodrugs

David B. Cohen

Georgia State University, davidbcohen47@gmail.com

Follow this and additional works at: https://scholarworks.gsu.edu/chemistry_theses

Recommended Citation

Cohen, David B., "Synthesis and Characterization of Carbon Monoxide Prodrugs." Thesis, Georgia State University, 2022.

doi: <https://doi.org/10.57709/29619586>

This Thesis is brought to you for free and open access by the Department of Chemistry at ScholarWorks @ Georgia State University. It has been accepted for inclusion in Chemistry Theses by an authorized administrator of ScholarWorks @ Georgia State University. For more information, please contact scholarworks@gsu.edu.

Synthesis and Characterization of Carbon Monoxide Prodrugs

by

David Benjamin Cohen

Under the direction of Binghe Wang, PhD

A Thesis Submitted in Partial Fulfillment of the Requirements for Degree of

Master of Science

in the College of Arts and Sciences

Georgia State University

2022

ABSTRACT

Carbon monoxide (CO) is an important endogenous signaling molecule that has pleiotropic effects through the regulation of a series of hemoprotein targets. It has been demonstrated repeatedly that there is a need for organic CO donors of various properties capable of the controlled release of CO since inhalation delivery has safety concerns and the reactivity and toxicity of metal-based donors are un-resolved issues. Our research group has previously described the synthesis and kinetic studies of organic CO prodrugs of various types with tunable release rates. In one series, the design makes use of an inverse-electron demand Diels-Alder cycloaddition, followed by a cheletropic reaction of the resulting norbornadienone intermediate to release CO. Herein, we describe the synthesis, characterization, and release kinetics of analogous CO prodrugs, with the aim of improved structural properties and/or release kinetics. These new CO prodrugs will add to the diverse set of CO donors available.

INDEX WORDS: Carbon monoxide, Prodrug, Tunable release rate, Norbornadienone

Copyright by
David Benjamin Cohen
2022

Synthesis and Characterization of Carbon Monoxide Prodrugs

by

David Benjamin Cohen

Committee Chair: Binghe Wang

Committee: Gigi Ray

Maged Henary

Electronic Version Approved:

Office of Graduate Services

College of Arts and Sciences

Georgia State University

August 2022

ACKNOWLEDGEMENTS

This is an incredibly surreal moment for me in my life, and it is hard knowing that no matter what I write here the words will not do my experience justice. I almost certainly would not have had the incredible experience that I did over the last three years were it not for the actions of my immediate mentors Dr. Kim Ladie de la Cruz, Dr. Xiaoxiao Yang, Dr. Manjusha Choudhury and soon-to-be Dr. Ravi Tripathi. You all mean the world to me and I certainly would not be the researcher or the person that I am now without you.

My experience in the Binghe Wang research group can really only be described as excellent, even when projects did not turn out the way they were intended, there were always jokes and laughs and good times occurring at every corner. I have made countless fond memories with my peers in this group and it is bittersweet to graduate and leave all the joking responsibilities to them. I know that Nicola Bauer, Shubham Bansal, Dongling Liu, Ce Yang, Tam Phat Nguyen, Ravi Tripathi, Rujuta Ghorpade, Shameer Kondengadan will certainly pick up the slack. It has meant so much to me to have been a part of such a diverse, hard-working, intelligent, and friendly team. There has never been a time when they have failed to put a big smile on my face, and for that I am incredibly grateful.

I could seriously go on forever and ever about all of the wonderful people who have touched my life along this journey, but I want to emphasize my committee in Dr. Maged Henary, Dr. Gigi Ray, and of course Dr. Binghe Wang. Dr. Wang has shown me time and time again what an exquisite leader he is and I was very lucky to be under his advisement. I cannot say enough good things about his character and his mentorship. He has actively shaped my professional self and for that I am eternally grateful.

Finally, the financial support that I received from my parents, Odie and Jeanne Cohen. Mom, dad, Jonathan, I do not know where I would be without you. Even if you never understood a thing I would come home and complain about, you were always there for me when my reactions would fail, or my kinetics experiments would keep me away until 4 AM. You would always be excited for me whenever my 'potions worked.' Your support and your love have certainly carried me to the finish line, and I cannot say thank you enough.

To all who have touched my life in one way or another, I am extremely grateful that you did. Your contributions have made me into the person that I am and will continue to shape me well into the future. We are all just the sum of our experience, and I am so blessed to have had such incredible people in my life. If you are still reading this far just know that you are so loved and everything that you are doing will be worth it. There is no such thing as bad experiences. At the same time, nothing, absolutely nothing is more important than your health, your happiness, and your safety. Live life to its fullest, and I hope you find what you are looking for.

TABLE OF CONTENTS

ACKNOWLEDGEMENTS	5
LIST OF TABLES	9
LIST OF FIGURES	10
LIST OF SCHEMES	11
1 INTRODUCTION.....	12
1.1 Protective Effects of Inhaled CO	12
1.2 CO Donors	13
1.3 Synthetic Design of New Prodrugs	20
1.4 Design of the Prodrug with an Internal Alkyne	20
1.5 Design of para-substituted electron withdrawing group and electron donating group	23
2 RESULTS AND DISCUSSION	23
2.1 Synthesis of CO Prodrugs	24
2.2 CO Release Rate	26
2.2.1 <i>Effect of Internal Alkyne on rate of CO release</i>	27
<i>Effect of electron withdrawing group and electron donating group</i>	28
2.2.2	28
3 EXPERIMENTAL PROCEDURES	29
4 REFERENCES.....	36

5	APPENDIX.....	40
----------	----------------------	-----------

LIST OF TABLES

Table 1. CO release rates from prodrugs.	27
---	----

LIST OF FIGURES

Figure 1. Structures of select CO-releasing molecules. Metal-based CO-RMs (CORM-1 and CORM-ALF186), boron-based CORM-A1, light-activated photoCO-RM, and enzyme triggered (ET-CORM) rac-1 and rac-4.	16
Figure 2. Structures of newly synthesized CO prodrugs.	20
Figure 3. Side-by-side structural comparison of CO prodrugs with a focus on the alkyne substitution pattern. All structures except BW-CO-138 have been previously reported..	22
Figure 4. From left to right: Structures of BW-CO-103, novel BW-CO-139, and novel BW-CO-140.....	23
Figure 5. Keto-enol tautomeric behavior seen in compounds 1a-c.	25

LIST OF SCHEMES

Scheme 1. Diels-Alder reaction between TPCPD and a strained alkyne to yield a norbornadienone intermediate (i) which undergoes a cheletropic reaction to release CO.	17
Scheme 2. Basic structural scaffold of the unimolecular organic prodrugs studied in this project and the position of varying substitution.....	18
Scheme 3. Comparison of the structural substitutions previously studied. The alkyne is shown in red and the carbonyl that is released as CO is shown in green. A) 5-membered ring formation is favored over 6-membered ring formation. B) Lactam formation is favored	19
Scheme 4.. General Synthetic Pathway for Unimolecular CO Prodrugs; Reagents and conditions: (i) pyridine, CH ₂ Cl ₂ , 0 °C-rt; (ii) amine or alcohol, toluene, heat; (iii) acenaphthylene-1,2-dione, DMF, Et ₃ N, rt; then Ac ₂ O, H ₂ SO ₄ , 0 °C; (iv) MeOH, reflux.	25

1 INTRODUCTION

Carbon monoxide (CO) owes its reputation as the “silent killer” due to its odorless and colorless appearance coupled with its ability to incapacitate and kill unsuspecting victims. It is widely documented that CO is toxic because of its ability to reversibly bind to the heme group of hemoproteins such as hemoglobin and myoglobin, interfering with oxygen transport and utilization throughout the body. CO also binds to cytochrome *c* oxidase, leading to inhibition of oxygen being reduced in the final step of the electron transport chain, halting aerobic respiration and oxidative phosphorylation.^{1,2} However, this first impression of CO provides an incomplete picture.

In the last several decades, we have experienced a CO renaissance. CO was discovered to be an endogenous signaling molecule, primarily produced at low levels by the enzyme heme oxygenase. This enzyme catalyzes the conversion of heme to CO and biliverdin, which is then converted into bilirubin by NADPH-dependent biliverdin reductase.^{3–5} At first, CO was only considered a waste byproduct, but in 1991 it was recognized that CO might play a role in physiological signaling.⁶ Since then, the field of studying CO as a potential therapeutic has blossomed; and it has been discovered that CO has a multitude of beneficial effects, including anti-inflammatory,^{7–14} anticancer,^{11,15–18} and cytoprotective benefits,^{11,12,19} among others.¹¹ The next section will describe these effects in more detail.

1.1 Protective Effects of Inhaled CO

There exists a plethora of demonstrated beneficial effects of inhaled CO. For example, in ex-smokers with diagnosed COPD, inhaled CO therapy was shown to improve responsiveness to methacholine and reduce sputum eosinophils.⁸ These human subjects were treated with 100-125 ppm CO for 2 hours per day for four consecutive days. Additionally, low-dose inhaled CO combined with intravenous resolvin D1 (an anti-inflammatory agent) was shown to specifically

reduce polymorphonuclear leukocyte (PMN)-mediated acute tissue injury in nonhuman primate (baboon) *Streptococcus pneumoniae* lung infection. This was demonstrated by the reduced amount of urinary cysteinyl leukotrienes consistent with lung protection.²⁰ The same study showed decreased PMN-platelet aggregates, decreased expression of adhesion molecules, and decreased expression of thromboxane B₂, in human whole blood treated with CO, all indicative of anti-inflammatory properties. Another study demonstrated that inhaled CO significantly reduced cardiopulmonary bypass-induced inflammation in pigs by the specific suppression of tumor necrosis factor α (TNF α) and interleukin-1 β .²¹ Furthermore, another study showed that gaseous CO reduced the generation of reactive oxygen species (ROS) resulting in the reduction of cellular injury in mice.²² Another research group demonstrated that inhaled CO exhibited antiproliferative effects of T-lymphocytes via the caspase-dependent pathway in mice.²³ Lastly, inhaled CO in pregnant women was shown to increase microvascular vasodilation suggesting that CO may be a potential therapeutic for preeclampsia.²⁴

With all of the demonstrated beneficial effects of CO, there have been attempts at finding alternative methods to deliver CO to suit various applications. While the most straightforward approach involves inhaled CO gas, there are safety and logistical concerns with the storage and manipulation of CO gas tanks, as well as a relative inability to control dosages through inhalation.²⁵ Alternatively, there have been several attempts at designing CO donors and prodrugs to release CO with some success. The next section will discuss some of these compounds in more detail.

1.2 CO Donors

There is a multitude of existing CO donors. These range from metal-based CO releasing molecules (CO-RMs), enzyme-triggered CO prodrugs (ET CO-RMs), metal and organic-based light-activated CO releasing-molecules (photoCO-RMs), and several scaffolds for fully organic

CO prodrugs. These different classes have been used for many biological studies with varying success, but each class comes with its own set of unique drawbacks. The following sections, as well as **Figure 1**, will describe these compounds in detail.

Perhaps the most well-known and most studied are the metal-based CO-RMs developed by the Motterlini group.^{26,27} For instance, tricarbonylchloro(glycinato)ruthenium(II) (CORM-3) is water soluble with a release rate that is pH-dependent.²⁸ The Motterlini group has demonstrated that CORM-3 can cause and sustain vasodilation in rats.²⁶ Additionally, they showed that CORM-3 promotes cardioprotection caused by hypoxia-reoxygenation and oxidative stress.²⁸ Also, CORM ALF-186 is a molybdenum-based CORM that has been shown to have anti-inflammatory and neuroprotective effects in retinal ganglion cells in rats.²⁹

Oftentimes included in conversations about metal-based CO-RMs is sodium boranocarbonate ($\text{Na}_2[\text{H}_3\text{BCO}_2]$), commonly referred to as CORM-A1 which is unique in that it does not feature a transition metal core. It has shown the ability to promote vasodilation³⁰ and was shown to inhibit metastasis of mammary-gland cancer in mice in early tumor development.³¹ This is to say that there are dozens of these metal-based CORMs. However, there are concerns about the toxic nature of the transition metal framework of these metal-based CORMs and their recently discovered chemical reactivity,^{32–35} prompting research into alternative methods of CO release.³⁶

Other CO-RMs have been developed as well with unique characteristics. These include enzyme-trigger CO releasing molecules (ET CO-RMs), which use an esterase enzyme to trigger CO release following oxidation.^{37,38} One potential benefit of enzyme-triggered release of CO is the increased ability to deliver CO intracellular rather than relying on gas diffusion across the cell membrane. Acyloxydiene- $\text{Fe}(\text{CO})_3$ complexes (named *rac-1* and *rac-2*) have been shown to

induce vasorelaxation of small mesenteric arteries in a pathway involving Kv7 potassium channels.³⁹

Additionally, photoactivated CO-releasing molecules (photoCO-RMs) have been developed. There exists metal-based photoCO-RMs⁴⁰ and completely organic variants as well. One example of the organic photoCO-RMs is 3-hydroxybenzo[g]flavone, which has demonstrated promising results as an anticancer and anti-inflammatory agent.⁴¹ However, as a therapeutic, photoCO-RMs will have difficulties in *in-vivo* studies of organs that are not readily accessible by light.

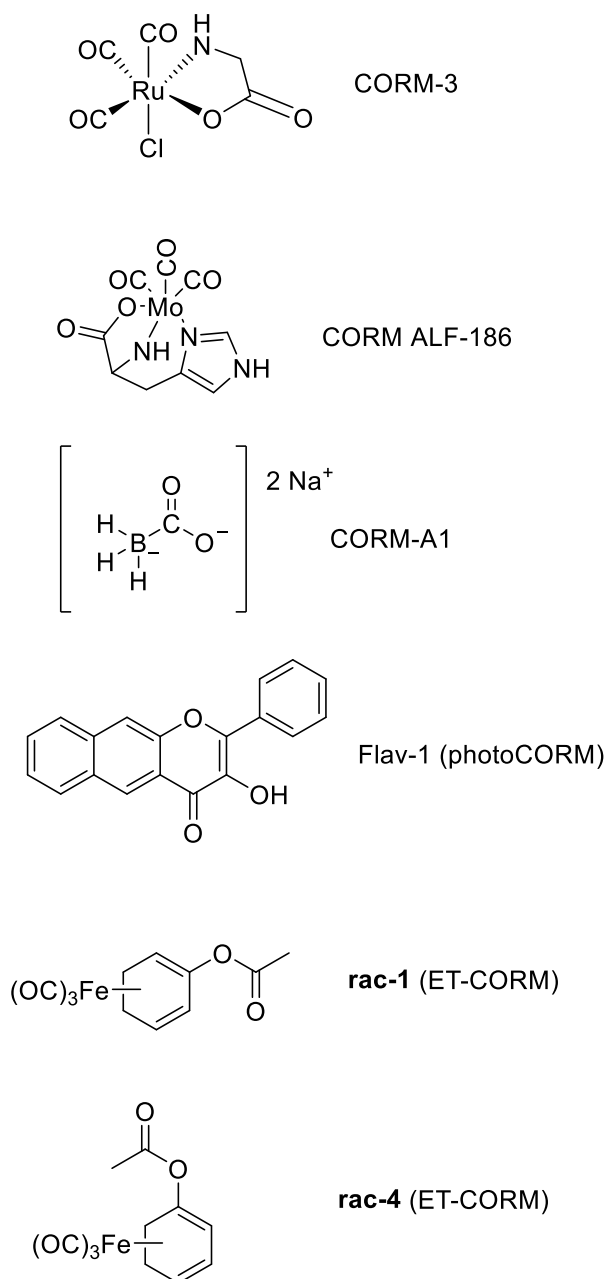
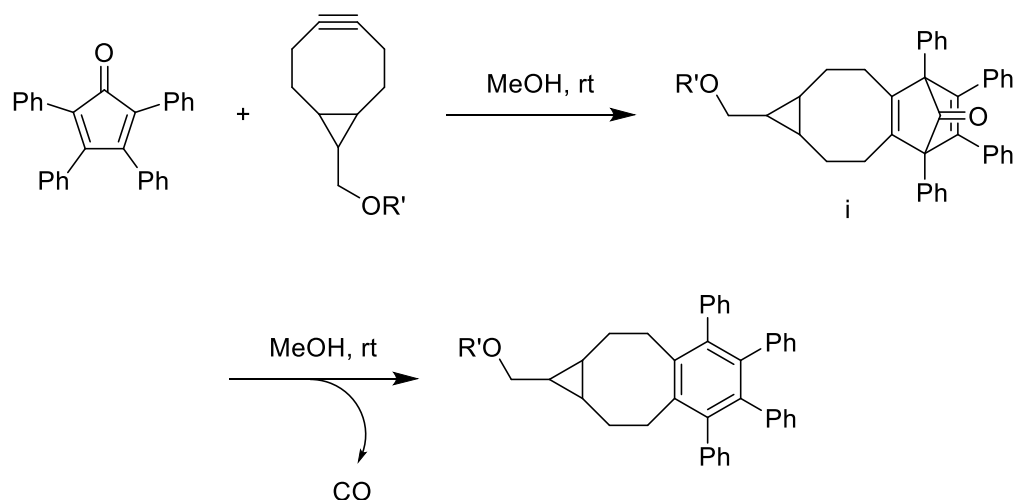


Figure 1. Structures of select CO-releasing molecules. Metal-based CO-RMs (CORM-1 and CORM-ALF186), boron-based CORM-A1, light-activated photoCO-RM, and enzyme triggered (ET-CORM) rac-1 and rac-4.

Over the last several years, our research group has produced several types of organic CO prodrugs by taking advantage of cheletropic reaction of norbornadienones. As shown in **Scheme 1**, a reaction between tetraphenylcyclopentadienone (TPCPD) and a strained alkyne was observed to release CO through the formation of a norbornadienone intermediate followed by a cheletropic

reaction at room temperature in methanol.^{42,43} The use of the strained alkyne was a novel idea in order to narrow the HOMO and LUMO energy gap to allow the initial Diels-Alder reaction at room temperature. However, a bimolecular click and release system introduces new challenges in a physiological environment, and in 2015 we introduced our unimolecular organic CO prodrugs.⁴⁴ It was hypothesized and then later demonstrated that the CO release rate of this unique class of CO prodrugs could be highly tunable, and there has been much study on this structure-rate release relationship.^{43–46}

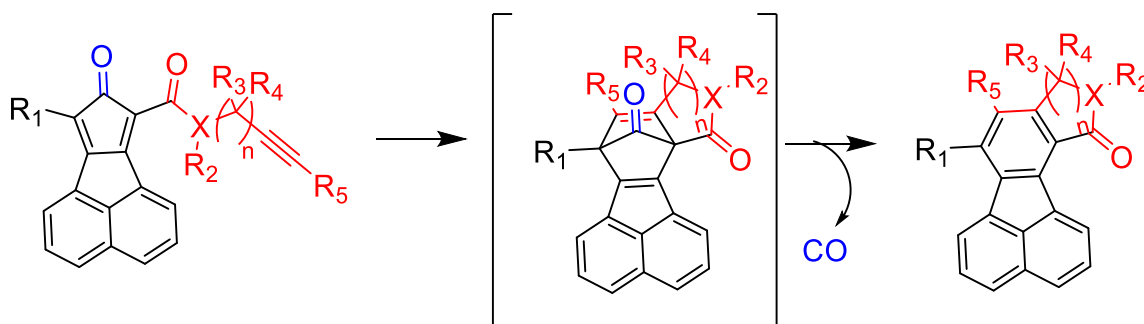


Scheme 1. Diels-Alder reaction between TPCPD and a strained alkyne to yield a norbornadienone intermediate (i) which undergoes a cheletropic reaction to release CO.

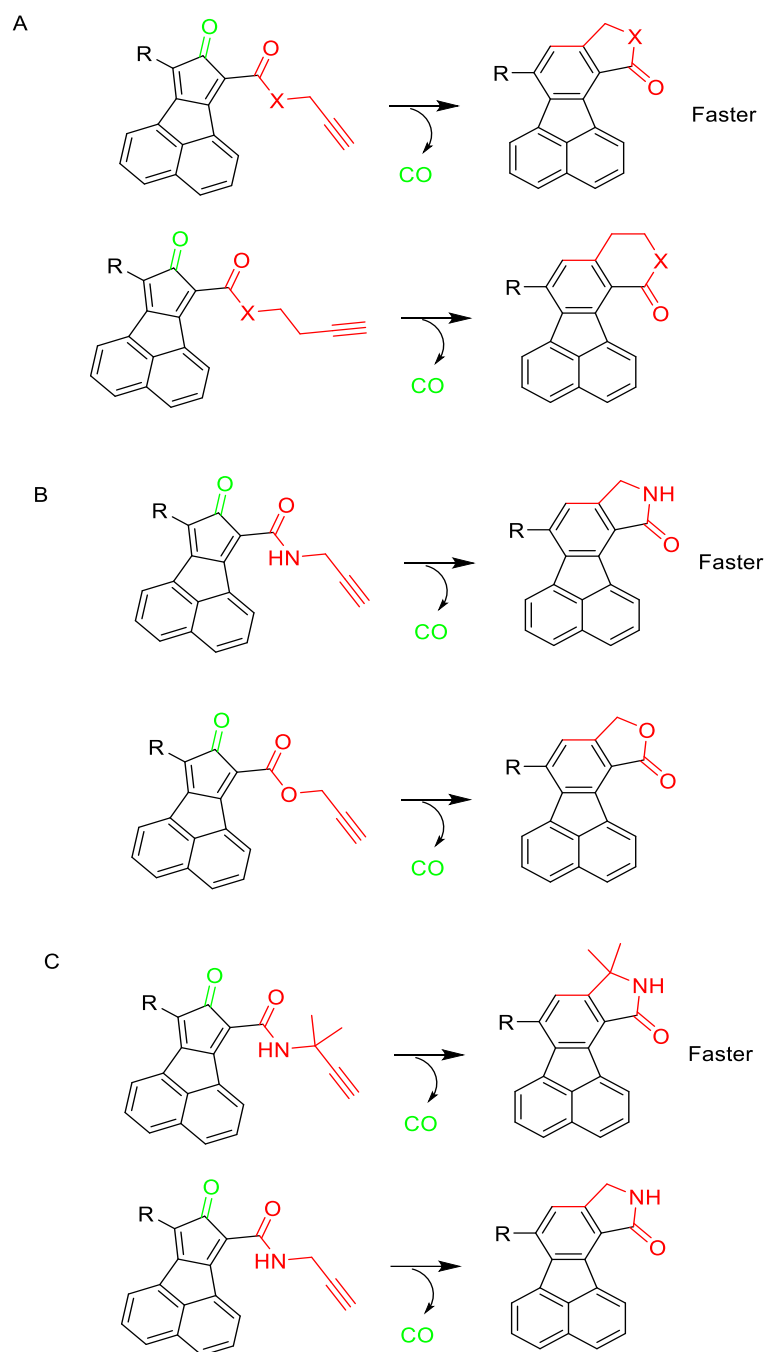
There are several positions on this class of prodrugs that allow for modifications, as shown in **Scheme 2**. The effects of some substitutions on the overall release rate of CO have been investigated.⁴⁶ For instance, previous studies have shown that the Diels-Alder reaction is favored if it leads to the formation of a 5-membered lactam or lactone involving the linker between the cyclopentadienone moiety and the tethered alkyne.⁴⁴ Additionally, the rate of CO release was observed to be much faster with an amide linker versus an ester linker. The introduction of the methyl group as R₃ and/or R₄ substituents to the propargylic linker portion greatly increased the

rate of CO release due to entropic effects.⁴⁶ Lastly, it has been shown that an internal alkyne leads to slower release rate of CO when compared to a terminal alkyne. A summary of these trends can be seen in **Scheme 3**. Herein, we will describe the synthesis and study of the release rates of three novel CO prodrugs and provide additional insights into the existing understanding of the structure rate-release relationships.

The first new compound was designed by adding a methyl group to the alkyne substituent in order to gain insight into the effect of this substitution pattern. The other new compounds were designed by altering the electronic properties of the substituents to vary the electron-donating or electron-withdrawing ability of the phenyl group. Such properties are known to affect the HOMO-LUMO energy gap and thus the kinetics of the rate-limiting Diels-Alder reaction.⁴² This study aims to investigate the effect of electron-donating groups (EDGs) and electron-donating groups (EWGs) as phenyl substituents on CO release rate, in order to further develop CO prodrugs as potential therapeutics and/or research tools.



Scheme 2. Basic structural scaffold of the unimolecular organic prodrugs studied in this project and the position of varying substitution.



Scheme 3. Comparison of the structural substitutions previously studied. The alkyne is shown in red and the carbonyl that is released as CO is shown in green. A) 5-membered ring formation is favored over 6-membered ring formation. B) Lactam formation is favored

1.3 Synthetic Design of New Prodrugs

Figure 2 details the structures of the newly synthesized and characterized prodrugs studied in this report. There were several goals in mind with the design of these compounds. Chiefly, we wanted to investigate the effect of new substitution patterns of these prodrugs compared to previously studied compounds to elucidate trends in CO release rate. Additionally, we wanted to develop more CO prodrugs with CO release in the 2-hour range, as we are lacking those compounds currently. With these goals in mind, **BW-CO-138** was designed with the specific goal of investigating the effect of a methyl substitution on the alkyne moiety on the CO release rate. **BW-CO-139** and **BW-CO-140** were designed with the goal of investigating the role of strong electron withdrawing group (EWG) and electron donating group (EDG) on the para-position of the phenyl group.

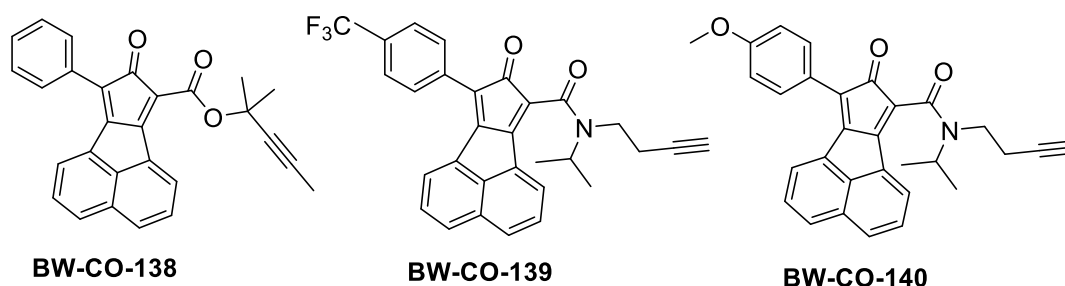


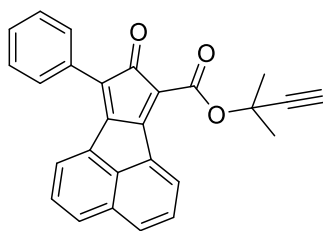
Figure 2. Structures of newly synthesized CO prodrugs.

1.4 Design of the Prodrug with an Internal Alkyne

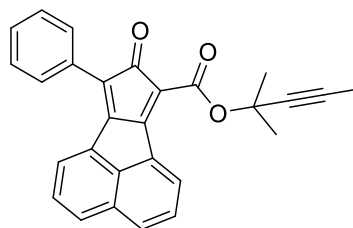
Figure 3 shows the structural comparison of previously reported **BW-CO-109** and novel **BW-CO-138**. These compounds are nearly the same, except for having a terminal and internal alkyne, respectively. It has already been established that the half-life for CO release for **BW-CO-109** is 33.0 ± 5.8 mins. Previous work⁴⁶ shows that **BW-CO-103** and **BW-CO-104**, which also

differ by this one feature, have CO release rates of 72 mins and 378 mins, respectively, showing that the internal alkyne reacts much more slowly than the terminal alkyne. If this trend were to continue, we would expect **BW-CO-138** to release CO with a significantly longer half-life than **BW-CO-109**, potentially in the 1-3 hours range, which would be a very useful analog and data point for our lab.

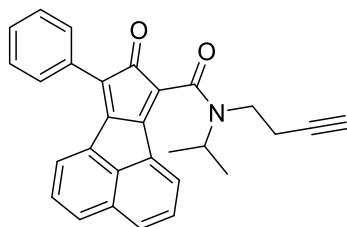
In previous studies,⁴⁶ substituents on the alkyne have shown to have varying effects on the rate of CO release. For example, previously studied compounds **BW-CO-101** and **BW-CO-102** were different in their structures in that **101** had a terminal alkyne while **102** had a bulky tert-butyl-diphenylsilyl (TBDPS) group in place of the terminal hydrogen, and there was no difference in rate release measured.⁴⁴ Finally, comparison of **BW-CO-108** (55.6 ± 1.45 hrs) and **BW-CO-127** (33.9 ± 1.35 hrs), where **127** has a triethyleneglycol attached directly to the alkyne shows the half-life for CO release from **127** is just over half of that for **BW-CO-108**.⁴⁵ From this set of data, it would seem that a methyl substituent on a terminal alkyne increases the half-life of CO release, but a strong EDG seems to decrease the half-life significantly.⁴⁶ **BW-CO-138** was made with the additional goal of further determining the effect of a methyl substituent on a terminal alkyne moiety.



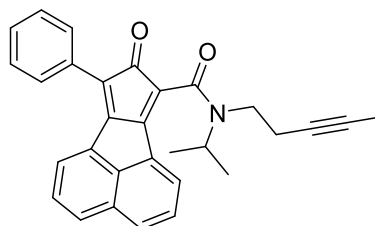
BW-CO-109



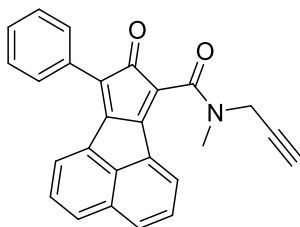
BW-CO-138



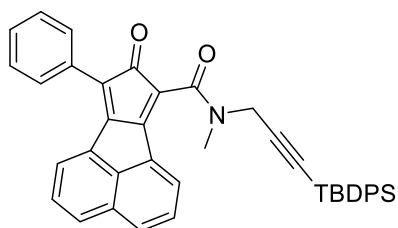
BW-CO-103



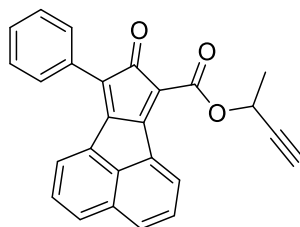
BW-CO-104



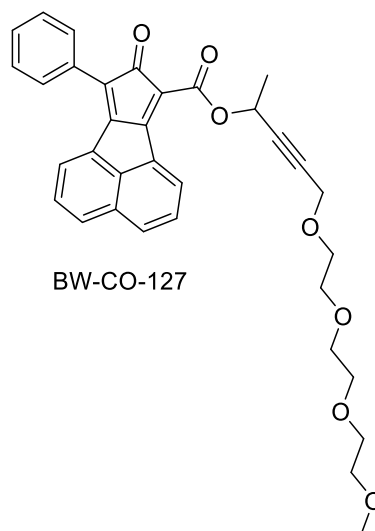
BW-CO-101



BW-CO-102



BW-CO-108



BW-CO-127

Figure 3. Side-by-side structural comparison of CO prodrugs with a focus on the alkyne substitution pattern. All structures except BW-CO-138 have been previously reported.

1.5 Design of para-substituted electron withdrawing group and electron donating group

Figure 4 shows the structures of **BW-CO-103**, a previously studied compound, compared with the newly designed **BW-CO-139** and **BW-CO-140**. It is well documented that the rate of Diels-Alder reactions is proportional to the size of the energy gap between the HOMO and LUMO orbitals. Other conformational and hydrophobic factors certainly come into play as well. In an inverse-electron demand Diels-Alder reaction seen in this class of CO prodrugs, the introduction of an EDG to the diene increases its LUMO energy while EWG introduction decreases its LUMO. As stated previously, the smaller the energy gap between the HOMO and LUMO, the faster the rate-determining Diels-Alder reaction can proceed. Notice the structural similarities of these compounds, which only differ in the presence of para-EWG and EDG, in **139** and **140**, respectively. The half-life of CO release for **BW-CO-103** has been previously measured to be 72 mins.⁴² The novel compounds were specifically designed with the goal of measuring the difference in CO release rates by the presence of these strong EWG and EDG.

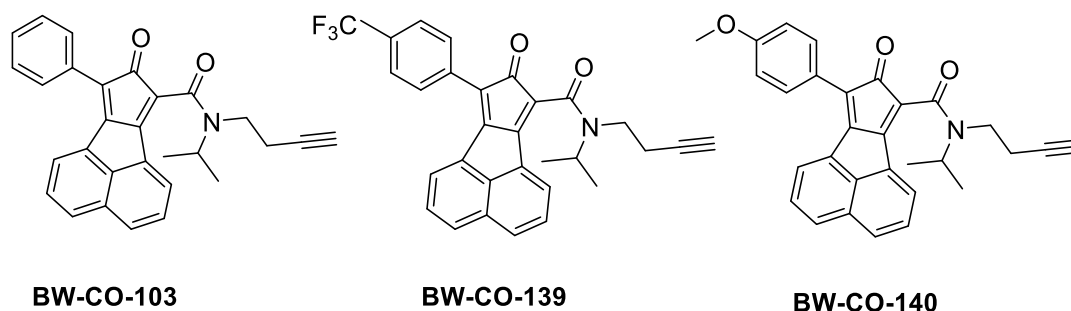


Figure 4. From left to right: Structures of BW-CO-103, novel BW-CO-139, and novel BW-CO-140.

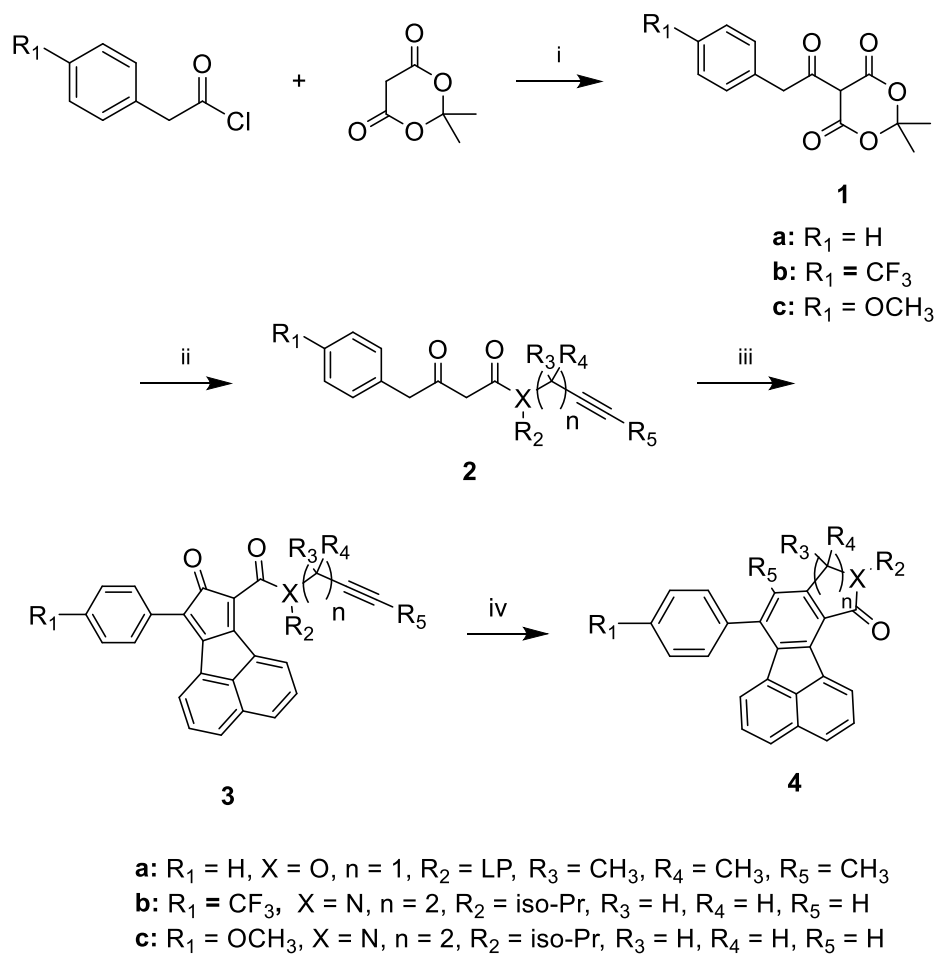
2 RESULTS AND DISCUSSION

The existing unimolecular organic CO prodrugs in this class function by using an intramolecular inverse-electron demand Diels-Alder reaction in which the diene (cyclopentadienone) and dienophile (alkyne) react to give an intermediate that undergoes a

subsequent cheletropic reaction to release CO spontaneously⁴³ (**Scheme 2**). Most notably, we have shown that the rate of CO release by these compounds is tunable with multiple positions of these prodrugs being tolerable of changes or substitutions or modifications. See the design of novel prodrugs section of the introduction. Briefly, we have noted in the past that the formation of a lactone versus a lactam, a five-membered versus a six-membered ring, the presence of an internal or terminal alkyne, and having substitutions on the alkyne wing all have drastic effects on the rate of CO release.⁴⁶ In this study, we determine how much the use of an internal alkyne, as well as the presence of EWG and EDG on the phenyl ring, change the rate of CO release under physiological conditions.

2.1 Synthesis of CO Prodrugs

The synthesis of these unimolecular CO prodrugs is detailed in **Scheme 4**. The synthetic method has been well established previously.^{43,46} Briefly, compounds **1a-c** were prepared from a nucleophilic acyl substitution reaction between Meldrum's acid and the appropriately substituted phenyl acetyl chloride (42-56%). This yield is lower than previously reported but can be explained by the slight decomposition of the Meldrum's acid stock that was used. Additionally, the behavior of compounds **1a-c** in column chromatography was unexpected based on TLC, as it was consistently found that the desired product moved slower than the starting material on TLC (hexane; EA and DCM; MeOH) but was eluted first in normal phase column chromatography. To date, our lab has not been able to explain this behavior. Also of note, these compounds were found to exist as stable enols in ¹H NMR. This can be explained by stable 6-membered hydrogen bonding that can occur in the enol form, as shown in **Figure 5** and explains the most downfield shift in ¹H NMR for these compounds (**1a-c**).



Scheme 4. General Synthetic Pathway for Unimolecular CO Prodrugs; Reagents and conditions: (i) pyridine, CH_2Cl_2 , $0\text{ }^{\circ}C$ -rt; (ii) amine or alcohol, toluene, heat; (iii) acenaphthylene-1,2-dione, DMF, Et_3N , rt; then Ac_2O , H_2SO_4 , $0\text{ }^{\circ}C$; (iv) MeOH, reflux.

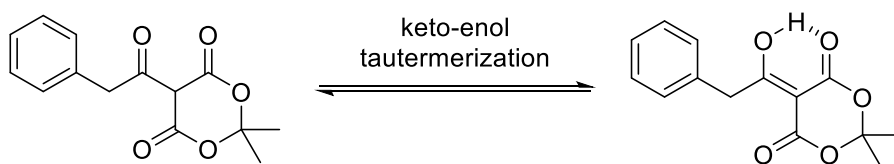


Figure 5. Keto-enol tautomeric behavior seen in compounds 1a-c.

Compounds **2a-c** were synthesized by reflux in toluene with the appropriate alcohol or amine. This reaction involves a nucleophilic attack on either ester carbonyl followed by a decarboxylation to yield CO₂ and acetone, as well as the targeted amide or ester. These products also were shown to exist in the enol form in ¹H NMR. Additionally, compounds **2b** and **2c** were shown to exist as rotamers.

Compounds **3a-c** were acquired through a double aldol condensation using triethyl amine (TEA) as a base. The TEA deprotonated an alpha carbon which allowed it to attack a carbonyl in acenaphthylene-1,2-dione, forming the beta-hydroxy-ketone product. This step then repeats to the second alpha carbon with the second carbonyl of acenaphthylene-1,2-dione to complete the formation of a five-membered ring. This intermediate was treated with H₂SO₄ to dehydrate both alcohols and form the necessary cyclopentadienone structure (63-33%). The resulting compound was purified with column chromatography and recrystallized from methanol to yield the target compounds **3a-c**. The lower yield typically occurs because of the cheletropic reaction to release CO and form the cyclized product is spontaneous and occurs in solution. ¹H NMR spectra show that compounds **3b** and **3c** exist as rotamers as well.

Finally, compounds **4a-c** were either isolated during the purification of **3a-c**, or **3a-c** were allowed to cyclize in hot methanol, concentrated under reduced pressure, and purified via column chromatography.

2.2 CO Release Rate

Following the synthesis of the three CO prodrugs, the rate of CO release was determined indirectly by monitoring the formation of the cyclized product (**4a-c**), which is fluorescent. Solutions between 50 μM and 100 μM were made of each prodrug. The fluorescence intensity of the solutions was measured at varying time points to determine the rate of formation of the cyclized

product as a surrogate indicator of the rate of CO release and subsequently the reaction rate constant as well as the half-life of each CO prodrug. The results, as well as the emission and excitation fluorescence information, can be found in **Table 1**.

Table 1. CO release rates from prodrugs.

<i>Prodrug</i>	<i>Rate Constant (min⁻¹)</i>	<i>t_{1/2} (min)</i>	<i>Emission Wavelength (nm)</i>	<i>Excitation Wavelength (nm)</i>
BW-CO-138	0.013 ± 0.0008	53.9 ± 3.2	457	378
BW-CO-139	0.0077 ± 0.0003	90.1 ± 3.4	457	322
BW-CO-140	0.0037 ± 0.0001	185.8 ± 5.9	459	376

2.2.1 Effect of Internal Alkyne on rate of CO release

BW-CO-138 was designed by introducing a methyl group on the terminal alkyne in order to slow the initial Diels-Alder reaction. It is well known that internal alkynes are less reactive in such Diels-Alder reactions.⁴⁰ Previous CO prodrugs **BW-CO-103** and **BW-CO-104** differ in this regard, and the rate of CO release observed in **BW-CO-104** was 6-fold slower as a result of the added methyl substituent. Thus, it was thought that since **BW-CO-138** was different from **BW-CO-109** ($t_{1/2} = 33.0 \pm 5.8$ mins) in the same regard, it should have a CO release half-life significantly longer than **BW-CO-109**. This was confirmed, as **BW-CO-138** was found to release CO with a half-life of 53.9 ± 3.2 mins. This shows that a methylated alkyne substitution pattern can be a very powerful tool to slow down CO release. More work could be done in the area to continue to fine-tune the CO release rate from these prodrugs.

2.2.2 *Effect of electron withdrawing group and electron donating group*

The main comparison to draw for the prodrugs **BW-CO-139** and **BW-CO-140** is the previously reported **BW-CO-103** ($t_{1/2} = 72$ mins).⁴⁴ Since the rate-limiting step of the CO release is the inverse electron demand Diels-Alder reaction, it was thought that the presence of a strong EWG on the electron-poor diene would speed up CO release by lowering LUMO energy, and a strong EDG would slow down CO release by raising the LUMO energy of the diene. However, this was found to not be the case, as both the para- CF_3 (**BW-CO-139**) and the para-methoxy (**BW-CO-140**) slowed down CO release. Specifically, **BW-CO-139** released CO with a half-life of 90.1 ± 3.4 mins, an increase of about 30% compared to **103**. Additionally, **BW-CO-140** was found to release CO with a half-life of 185.8 ± 5.9 mins, almost 2.5 times slower. Between the two new prodrugs, indeed the one with an EDG (**BW-CO-140**) was found to have a slower release rate than the one with an EWG (**BW-CO-139**).

This observed trend between **BW-CO-139** and **140** may be explained by the differences in the HOMO-LUMO energy gap as a contributing factor. However, other factors such as the hydrophobicity of the diene portion, and/or conformational constraints are known to play important roles in controlling reaction rates.⁴⁶ More studies are needed to understand the effects on the rate of CO release of this substitution at this para-position on the para-position on the phenyl ring on the diene.

As expected, the rate of CO release from **BW-CO-140** is much slower than its non-substituted counterpart (**BW-CO-103**). This can be explained by the proposed increase in the LUMO energy of the cyclopentadienone. As stated previously, the larger the energy gap between HOMO and LUMO, the slower the Diels-Alder reaction will occur. The methoxy-substituted phenyl group of the diene could be a powerful tool to slow the rate of CO release appreciably.

Conclusion

Three novel CO prodrugs were synthesized, characterized, and their CO release rates were determined. The modifications made were done specifically to determine the effect on CO release rate by these unexplored substitutions. It was found that the modification of a terminal alkyne to an internal alkyne by way of a methyl group introduction increases the half-time of CO release, but the temporal difference may also be dependent on other structural variables as well. These include the characteristics of the linker as well as the nature of the linker connection.

Additionally, the introduction of a methoxy (EDG) or $-\text{CF}_3$ (EWG) on the diene was shown to increase the half-life of CO release, further supporting the notion that this scaffold is highly tunable. The results also show that the effect of the substitution is more than a simple electronic effect in a traditional sense, which normally anticipates that an EWG on the diene would lower the LUMO energy leading to the narrowing of the LUMO-HOMO gap for reaction rate acceleration. Though the goal of substitution to speed up CO release rate was not met, the information gained will aid future work. Furthermore, a vast challenge in studying our CO prodrugs *in vivo* is solubility. In this study, we have shown that this scaffold tolerates well substituents with varying electronic properties, potentially allowing for the future introduction of hydrophilic substitution patterns. These substitutions would be most beneficial in increasing the solubility of these compounds, aiding our effort to study *in vivo* effects.

3 EXPERIMENTAL PROCEDURES

Starting materials were purchased from Sigma-Aldrich or Oakwood Chemicals and were directly used without further purification. All solvents used in experiments were purchased from

Thermo Fisher Scientific. Anhydrous solvents were used for all moisture-sensitive reactions. Column chromatography was carried out using flash silica gel (Sorbent 230–400 mesh). TLC analysis was conducted on silica gel plates (Sorbent Silica G UV254). Compounds were dried under 5 mm Hg vacuum. ^1H and ^{13}C NMR spectra were recorded on an Avance Bruker 400 NMR spectrometer using deuterated solvent. MS was analyzed by the Georgia State University Mass Spectrometry Facilities using (ESI)+ or (ESI)- method. **Scheme 4** details the overall synthetic scheme for this class of CO prodrugs.

Synthesis of Compound 1a-c

Meldrum's acid (3.47 mmol, 1 equiv) was dissolved in dry DCM and chilled to 0 °C. Then, pyridine (6.94 mmol, 2 equiv) was added dropwise, followed by phenyl acetyl chloride or the appropriate derivative (1.2 eq). The reaction was warmed to room temperature and stirred for 3 hours. Then the reaction was quenched with 5% HCl, washed with brine, dried over anhydrous Na_2SO_4 , and finally concentrated under reduced pressure. The reaction mixture was then purified by flash column chromatography (hexane: ethyl acetate gradient) to yield the crude product, which was then recrystallized from ether and hexane to yield the pure compound.

1a, 2,2-Dimethyl-5-(2-phenylacetyl)-1,3-dioxane-4,6-dione*: White solid; yield: 55%. ^1H NMR (CDCl_3): δ 15.35 (s, 1 H), 7.44 – 7.29 (m, 5 H), 4.45 (s, 2 H), 1.74 (s, 6 H).⁴⁶

1b, 2,2-Dimethyl-5-(2-(4-(trifluoromethyl)phenyl)acetyl)-1,3-dioxane-4,6-dione: White solid; yield 47%; ^1H NMR (CDCl_3) δ 15.38 (s, 1H), 7.59 (d, J = 8.2 Hz, 2H), 7.52 (d, J = 8.1 Hz, 2H), 7.26 (s, 1H), 4.47 (s, 2H), 1.73 (s, 6H). ^{13}C NMR (CDCl_3): δ 193.3, 170.5, 138.0,

130.0, 125.6, 124.3, 115.0, 111.8, 105.3, 40.6, 26.9. HRMS (ESI)⁻ calculated for C₁₅H₁₂O₅F₃ [M-H]⁺: m/z 329.0637, found 329.0644.

1c, 5-(2-(4-Methoxyphenyl)acetyl)-2,2-dimethyl-1,3-dioxane-4,6-dione: White solid (yield 42%). ¹H NMR (CDCl₃): δ 15.30 (s, 1 H), 7.32 (d, *J* = 12 Hz, 2 H), 6.86 (d, *J* = 12 Hz, 2 H), 4.35 (s, 2 H), 3.78 (s, 3 H) 1.71 (s, 6 H). ¹³C NMR (CDCl₃) δ 199.9, 158.2, 130.8, 128.6, 116.1, 113.7, 103.1, 89.9, 55.4, 46.7, 26.0 (ESI)⁻ calculated for C₁₅H₁₆O₆ [M-H]⁺: m/z 291.0869, found 291.0878.

Synthesis of Compounds 2a-c

Compound **1** (10.4 mmol) was dissolved in toluene (10 mL), and the appropriate amine or alcohol (1.5 eq) was added in a sealed container. The reaction mixture was heated gradually (over 10 minutes) to 110 °C while stirring. Once the reaction mixture reached 110 °C, it was left to stir for 4 hours. The crude product was concentrated under rotary evaporation and then purified via silica gel chromatography (8:1 Hexane EA) to give the pure compound.

2a, 2-Methylpent-3-yn-2-yl 3-oxo-4-phenylbutanoate: Clear oil (yield 78%). ¹H NMR (CDCl₃) δ 7.37 – 7.27 (m, 3H), 7.21 (d, *J* = 7.1 Hz, 2H), 3.77 (s, 2H), 3.45 (s, 2H), 1.84 (s, 3H), 1.66 (d, *J* = 13.8 Hz, 6H). ¹³C NMR (CDCl₃) δ 200.7, 165.6, 133.5, 129.7, 128.9, 127.4, 81.0, 80.0, 74.3, 49.9, 49.3, 29.2, 3.8. HRMS (ESI)⁻ calculated for C₁₆H₁₈O₃ [M-H]⁻: m/z 257.1178, found 257.1177.

2b, N-(But-3-yn-1-yl)-N-isopropyl-3-oxo-4-(4-(trifluoromethyl)phenyl)butanamide: Light brown oil (yield 55%). ¹H NMR (CDCl₃) 15.01 (s, 1H), 7.59 (d, *J* = 7.4 Hz, 2H), 7.38 (dd, *J* = 18.7, 7.8 Hz, 2H), 4.83 (dd, *J* = 180.4, 74.4 Hz, 1H), 4.05 – 3.75 (m, 2H), 3.58 (d, *J* = 20.0 Hz, 2H), 3.45 – 3.19 (m, 2H), 2.45 (d, *J* = 48.3 Hz, 2H), 2.01 (d, *J* = 17.9 Hz, 1H), 1.18 (dd, *J* = 18.6,

6.7 Hz, 6H). ^{13}C NMR (CDCl_3): δ 201.34, 166.14, 137.73, 130.23, 129.65, 125.71, 81.74, 70.03, 49.56, 49.39, 48.93, 40.34, 21.23, 18.60. HRMS (ESI) $^+$ calculated for $\text{C}_{18}\text{H}_{20}\text{F}_3\text{NO}_2$ $[\text{M}+\text{H}]^+$: m/z 340.1524, found 340.1525.

2c, *N*-(But-3-yn-1-yl)-*N*-isopropyl-4-(4-methoxyphenyl)-3-oxobutanamide: Light brown oil (yield 68%). 14.97 (d, J = 36 Hz, 1 H), 7.16 (dd, J = 17.4, 8.4 Hz, 2H), 6.87 (d, J = 8.5 Hz, 2H), 3.79 – 3.68 (m, 4H), 3.50 (dd, J = 40.5, 8.5 Hz, 2H), 3.38 – 3.21 (m, 2H), 2.60 – 2.40 (m, 1H), 2.33 (dd, J = 14.0, 7.2 Hz, 1H), 1.88 (t, J = 77.6 Hz, 2H), 1.13 (dd, J = 18.0, 10.0 Hz, 6H). ^{13}C NMR (CDCl_3): δ 202.19, 166.23, 159.00, 130.59, 125.76, 114.35, 81.82, 69.63, 55.24, 49.33, 48.93, 48.38, 40.26, 21.03, 20.25, 18.59. HRMS (ESI) $^+$ calculated for $\text{C}_{18}\text{H}_{23}\text{NO}_3$ $[\text{M}+\text{H}]^+$: m/z 302.1756, found 302.1764.

Synthesis of Compounds 3a-c

Compound **2** (0.58 mmol, 1 eq) and acenaphthalene-1,2-dione (1.01 eq) were dissolved in 5 mL of DMF, and then TEA (1.5 eq) was added. The reaction mixture was stirred for 1.5 hours, then concentrated under reduced pressure. The resulting residue was dissolved in a minimum amount of acetic anhydride, chilled to 0 °C, and treated with 2-3 drops of concentrated H_2SO_4 . The solution was stirred for 10 minutes, then diluted with ethyl acetate, and was finally washed with NaHCO_3 solution three times. The organic layer was then washed with brine thrice, and finally was dried over Na_2SO_4 , and then concentrated under reduced pressure. The residue was then purified by silica gel chromatography in 10:1 Hexane: EA to obtain the crude product. The crude product was recrystallized from MeOH to yield dark solids.

3a, 2-Methylpent-3-yn-2-yl 8-oxo-9-phenyl-8H-cyclopenta[a]acenaphthylene-7-carboxylate, BW-CO-138: Dark solid with green flecks (yield 33%). ^1H NMR (400 MHz, CDCl_3) δ 8.86 (d, $J = 7.2$ Hz, 1H), 8.02 (dd, $J = 9.9, 7.7$ Hz, 2H), 7.90 (d, $J = 8.2$ Hz, 1H), 7.80 (d, $J = 7.2$ Hz, 2H), 7.78 – 7.71 (m, 1H), 7.64 – 7.56 (m, 1H), 7.51 (t, $J = 7.5$ Hz, 2H), 7.43 (t, $J = 7.4$ Hz, 1H), 1.90 (s, 3H), 1.87 (s, 6H). ^{13}C NMR (CDCl_3) δ 196.8, 169.3, 160.9, 150.6, 144.8, 131.4, 130.5, 130.2, 130.0, 129.4, 128.8, 128.4, 128.1, 127.6, 123.7, 121.0, 110.9, 80.6, 73.4, 29.4, 3.7. HRMS (ESI) $^+$ showed the CO release product, calculated for $\text{C}_{27}\text{H}_{20}\text{O}_2$ $[\text{M}+\text{H}]^+$: m/z 377.1542, found 377.1547.

3b, N-(But-3-yn-1-yl)-N-isopropyl-8-oxo-9-(4-(trifluoromethyl)phenyl)-8H-cyclopenta[a]acenaphthylene-7-carboxamide, BW-CO-139: Dark Purple solid (yield 63%). ^1H NMR (CDCl_3) 7.99 (d, $J = 7.1$ Hz, 1H), 7.97 – 7.87 (m, 5H), 7.77 (d, $J = 8.2$ Hz, 2H), 7.64 (dt, $J = 22.4, 7.7$ Hz, 2H), 4.84 – 3.96 (m, 1H), 3.59 (t, $J = 9.6$ Hz, 2H), 2.69 (t, $J = 8.0$ Hz, 2H), 2.15 – 1.81 (s, 1H), 1.25 (d, $J = 6.6$ Hz, 6H). ^{13}C NMR (CDCl_3): δ 198.6, 164.1, 162.0, 154.3, 145.3, 134.6, 132.1, 130.7, 130.2, 129.9, 129.4, 129.3, 129.1, 128.7, 125.7, 124.1, 121.7, 120.9, 120.6, 117.4, 82.1, 70.1, 52.0, 40.2, 21.8, 18.7. HRMS (ESI) $^+$ calculated for $\text{C}_{30}\text{H}_{22}\text{F}_3\text{NO}_2$ $[\text{M}+\text{H}]^+$: m/z 486.1681, found 486.1704.

3c; N-(But-3-yn-1-yl)-N-isopropyl-9-(4-methoxyphenyl)-8-oxo-8H-cyclopenta[a]acenaphthylene-7-carboxamide, BW-CO-140: Dark solid with yellow green tint (yield 45%). ^1H NMR (CDCl_3) δ 7.98 (d, $J = 7.1$ Hz, 1H), 7.96 – 7.89 (m, 2H), 7.85 (d, $J = 8.2$ Hz, 1H), 7.76 (d, $J = 8.7$ Hz, 2H), 7.61 (dt, $J = 22.9, 7.7$ Hz, 2H), 7.05 (d, $J = 8.8$ Hz, 2H), 4.12 (dt, $J = 13.1, 6.5$ Hz, 1H), 3.89 (s, 3H), 3.64 – 3.51 (m, 2H), 2.66 (dd, $J = 61.3, 54.9$ Hz, 2H), 1.96 (d, $J = 90.0$ Hz, 1H), 1.24 (d, $J = 6.6$ Hz, 6H). ^{13}C NMR (CDCl_3): δ 199.6, 164.5, 160.7, 160.2, 148.6, 145.0, 132.0, 131.5, 130.8, 130.3, 129.1, 128.8, 127.5, 123.9, 123.5, 122.2, 120.9, 116.6,

114.4, 82.2, 70.0, 55.5, 40.1, 21.8, 18.7. HRMS (ESI)⁺ calculated for C₃₀H₂₅NO₃ [M+H]⁺: m/z 448.1913, found 448.1928.

Synthesis of Compounds 4a-c

During the column chromatography and recrystallization of **3a-c**, impure mixtures contaminated with **4a-c** (the cyclized product following CO release) were collected. These fractions were redissolved in methanol and heated under reflux for 6 hours in order to allow for full conversion to the cyclized product. Concentration under reduced pressure followed by column chromatography yielded pure target compound.

4a, 3,3,4-Trimethyl-5-phenylfluorantheno[7,8-c]furan-1(3H)-one, BW-CP-138: Yellow solid.

¹H NMR (CDCl₃): δ 9.22 (d, *J* = 7.1 Hz, 1H), 7.91 (d, *J* = 8.1 Hz, 1H), 7.81 – 7.71 (m, 2H), 7.68 – 7.54 (m, 3H), 7.42 – 7.34 (m, 2H), 7.32 – 7.27 (m, 1H), 6.41 (d, *J* = 7.1 Hz, 1H), 2.25 (s, 3H), 1.87 (s, 6H). ¹³C NMR (CDCl₃): δ 170.1, 151.8, 144.3, 139.5, 139.28, 135.7, 134.0, 132.8, 129.6, 129.5, 128.9, 128.8, 128.7, 128.4, 128.3, 128.0, 127.9, 127.6, 127.4, 123.8, 120.5, 87.0, 26.23, 16.0. HRMS (ESI)⁺ calculated for C₂₇H₂₀O₂ [M+H]⁺: m/z 377.1542, found 377.1547.

4b, 2-Isopropyl-6-(4-(trifluoromethyl)phenyl)-3,4-dihydroacenaphtho[1,2-h]isoquinolin-1(2H)-one, BW-CP-139: Yellow solid. ¹H NMR (CDCl₃) δ 9.25 (d, *J* = 7.3 Hz, 1H), 7.88 (d, *J* = 8.1 Hz, 1H), 7.81 (dd, *J* = 8.1, 3.0 Hz, 3H), 7.71 (t, *J* = 7.8 Hz, 3H), 7.34 (t, *J* = 7.6 Hz, 1H), 7.08 – 6.95 (m, 2H), 5.26 (dd, *J* = 13.6, 6.8 Hz, 1H), 3.62 – 3.40 (m, 2H), 3.04 (t, *J* = 6.1 Hz, 2H), 1.30 (d, *J* = 6.5 Hz, 6H). ¹³C NMR (CDCl₃) δ 163.6, 150.6, 139.8, 139.5, 139.3, 138.9, 138.5, 138.1, 137.1, 136.1, 135.2, 135.1, 134.9, 133.5, 131.3, 129.5, 129.0, 128.1, 127.6, 127.1, 126.1, 125.7, 123.9, 122.4, 111.3, 76.8, 41.7, 38.8, 34.7, 30.7, 29.8, 20.2, 17.2. HRMS (ESI)⁺ calculated for C₂₉H₂₂F₃NO [M+H]⁺: m/z 458.1732, found 458.1729.

4c, 2-Isopropyl-6-(4-methoxyphenyl)-3,4-dihydroacenaphtho[1,2-h]isoquinolin-1(2H)-one, BW-CP-140

^1H NMR (400 MHz, CDCl_3) δ 9.25 (d, J = 7.3 Hz, 1H), 7.86 (d, J = 8.1 Hz, 1H), 7.77 (d, J = 8.1 Hz, 1H), 7.69 (t, J = 7.7 Hz, 1H), 7.48 (d, J = 8.6 Hz, 2H), 7.33 (t, J = 7.6 Hz, 1H), 7.14 (d, J = 7.1 Hz, 1H), 7.10 – 7.00 (m, 3H), 5.34 – 5.18 (m, 1H), 3.93 (s, 3H), 3.55 – 3.42 (m, 2H), 3.00 (t, J = 6.1 Hz, 2H), 1.29 (d, J = 6.8 Hz, 6H). ^{13}C NMR (CDCl_3) δ 163.9, 159.6, 140.8, 139.7, 138.3, 137.6, 135.6, 133.3, 133.0, 130.1, 129.7, 129.3, 128.4, 128.0, 127.7, 127.2, 126.9, 126.1, 122.6, 114.1, 55.5, 44.0, 38.8, 30.7, 20.2. HRMS (ESI) $^+$ calculated for $\text{C}_{29}\text{H}_{25}\text{NO}_2$ $[\text{M}+\text{H}]^+$: m/z 420.1964, found 420.1950.

General Procedure for CO Release Kinetics

Fluorescence studies were carried out using a SHIMADZU RF-5310PC with slit width for excitation and emission at 5 nm. Appropriate excitation and emission wavelengths were found by making solutions of 50-100 μM of the **CP** compounds (**4a-c**). An emission scan with an excitation wavelength at 365 nm was taken to find the maximum emission wavelength. Then, using the newfound emission wavelength, an appropriate excitation wavelength was determined. These optimized emission and excitation wavelengths were used to measure the rate of CO release

The cyclization studies were done by making 50-100 μM solutions of the CO compound in 5:1 DMSO:PBS buffer, and incubating them at 37 $^\circ\text{C}$. Then, a multitude of fluorescence scans were taken at varying time intervals. The raw data can be found in the appendix.

4 REFERENCES

- (1) Alonso, J.-R.; Cardellach, F.; López, S.; Casademont, J.; Miró, Ò. Carbon Monoxide Specifically Inhibits Cytochrome C Oxidase of Human Mitochondrial Respiratory Chain. *Pharmacol. Toxicol.* **2003**, *93* (3), 142–146.
- (2) Blumenthal, I. Carbon Monoxide Poisoning. *J. R. Soc. Med.* **2001**, *94* (6), 270–272.
- (3) Tenhunen, R.; Marver, H. S.; Schmid, R. Microsomal Heme Oxygenase. *J. Biol. Chem.* **1969**, *244* (23), 6388–6394.
- (4) Tenhunen, R.; Marver, H. S.; Schmid, R. The Enzymatic Conversion of Heme to Bilirubin by Microsomal Heme Oxygenase. *Proc. Natl. Acad. Sci. U. S. A.* **1968**, *61* (2), 748–755.
- (5) Araujo, J.; Zhang, M.; Yin, F. Heme Oxygenase-1, Oxidation, Inflammation, and Atherosclerosis. *Front. Pharmacol.* **2012**, *3*.
- (6) Marks, G., S.; Brien, J., F.; Nakatsu, K.; McLaughlin, B., E. Does carbon monoxide have a physiological function? *Trend. Pharmacol. Sci.* **1991**, *12*, 185–188.
- (7) Otterbein, L. E.; Bach, F. H.; Alam, J.; Soares, M.; Tao Lu, H.; Wysk, M.; Davis, R. J.; Flavell, R. A.; Choi, A. M. K. Carbon Monoxide Has Anti-Inflammatory Effects Involving the Mitogen-Activated Protein Kinase Pathway. *Nat. Med.* **2000**, *6* (4), 422–428.
- (8) Bathoorn, E.; Slebos, D.-J.; Postma, D. S.; Koeter, G. H.; van Oosterhout, A. J. M.; van der Toorn, M.; Boezen, H. M.; Kerstjens, H. A. M. Anti-Inflammatory Effects of Inhaled Carbon Monoxide in Patients with COPD: A Pilot Study. *Eur. Respir. J.* **2007**, *30* (6), 1131–1137.
- (9) Slebos, D.-J.; Ryter, S. W.; Choi, A. M. Heme Oxygenase-1 and Carbon Monoxide in Pulmonary Medicine. *Respir. Res.* **2003**, *4* (1), 7.
- (10) Chapman, J. T.; Otterbein, L. E.; Elias, J. A.; Choi, A. M. Carbon monoxide attenuates aeroallergen-induced inflammation in mice. *Am. J. Physiol. Lung. Cell. Mol. Physiol.* **2001**, *281*(1), L209–216.
- (11) Gullotta, F.; Masi, A. di; Ascenzi, P. Carbon Monoxide: An Unusual Drug. *IUBMB Life* **2012**, *64* (5), 378–386.
- (12) Nakao, A.; Choi, A. M. K.; Murase, N. Protective Effect of Carbon Monoxide in Transplantation. *J. Cell. Mol. Med.* **2006**, *10* (3), 650–671.
- (13) Fredenburgh, L. E.; Kraft, B. D.; Hess, D. R.; Harris, R. S.; Wolf, M. A.; Suliman, H. B.; Roggli, V. L.; Davies, J. D.; Winkler, T.; Stenzler, A.; Baron, R. M.; Thompson, B. T.; Choi, A. M.; Welty-Wolf, K. E.; Piantadosi, C. A. Effects of Inhaled CO Administration on Acute Lung Injury in Baboons with Pneumococcal Pneumonia. *Am. J. Physiol. - Lung Cell. Mol. Physiol.* **2015**, *309* (8), L834–L846.
- (14) Bakalarz, D.; Surmiak, M.; Yang, X.; Wójcik, D.; Korbut, E.; Śliwowski, Z.; Ginter, G.; Buszewicz, G.; Brzozowski, T.; Cieszkowski, J.; Głowacka, U.; Magierowska, K.; Pan, Z.; Wang, B.; Magierowski, M. Organic Carbon Monoxide Prodrug, BW-CO-111, in Protection against Chemically-Induced Gastric Mucosal Damage. *Acta Pharm. Sin. B* **2021**, *11* (2), 456–475.
- (15) Vitek, L.; Gbelcová, H.; Muchová, L.; Váňová, K.; Zelenka, J.; Koníčková, R.; Šuk, J.; Zadinova, M.; Knejzlík, Z.; Ahmad, S.; Fujisawa, T.; Ahmed, A.; Ruml, T. Antiproliferative Effects of Carbon Monoxide on Pancreatic Cancer. *Dig. Liver Dis.* **2014**, *46* (4), 369–375.

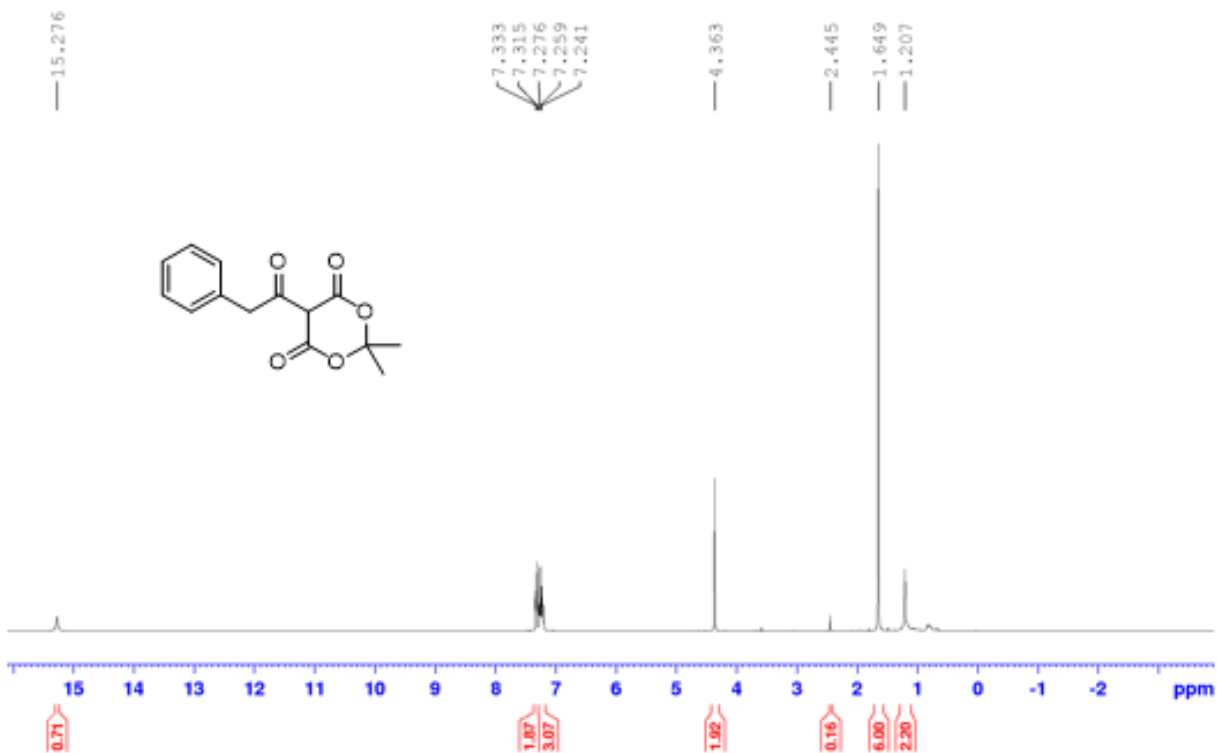
- (16) Huang, C.-C.; Ho, C.-H.; Chen, Y.-C.; Hsu, C.-C.; Lin, H.-J.; Tian, Y.-F.; Wang, J.-J.; Guo, H.-R. Impact of Carbon Monoxide Poisoning on the Risk of Breast Cancer. *Sci. Rep.* **2020**, *10* (1), 20450.
- (17) Zhu, X.; Fan, W.-G.; Li, D.-P.; Lin, M. C.; Kung, H. Heme Oxygenase-1 System and Gastrointestinal Tumors. *World J. Gastroenterol. WJG* **2010**, *16* (21), 2633–2637.
- (18) Wegiel, B.; Gallo, D.; Csizmadia, E.; Harris, C.; Belcher, J.; Vercellotti, G. M.; Penacho, N.; Seth, P.; Sukhatme, V.; Ahmed, A.; Pandolfi, P. P.; Helczynski, L.; Bjartell, A.; Persson, J. L.; Otterbein, L. E. Carbon Monoxide Expedites Metabolic Exhaustion to Inhibit Tumor Growth. *Cancer Res.* **2013**, *73* (23).
- (19) Santoro, G.; Beltrami, R.; Kottelat, E.; Blacque, O.; Bogdanova, A. Yu.; Zobi, F. N-Nitrosamine- $\{cis-Re[CO]_2\}^{2+}$ Cobalamin Conjugates as Mixed CO/NO-Releasing Molecules. *Dalton Trans.* **2016**, *45* (4), 1504–1513.
- (20) Shinohara Masakazu; Kibi, M.; Riley, I. R.; Chinag, N.; Dalli, J.; Kraft, B. D.; Piantadosi, C. A.; Choi, A. M. K.; Serhan, C. N. Cell-Cell Interactions and Bronchoconstrictor Eicosanoid Reduction with Inhaled Carbon Monoxide and Resolvin D1. *Am. J. Physiol. - Lung Cell. Mol. Physiol.* **307**, L746–L757.
- (21) Goebel, U.; Siepe, M.; Mecklenburg, A.; Stein, P.; Roesslein, M.; Schwer, C. I.; Schmidt, R.; Doenst, T.; Geiger, K. K.; Pahl, H. L.; Schlensak, C.; Loop, T. Carbon Monoxide Inhalation Reduces Pulmonary Inflammatory Response during Cardiopulmonary Bypass in Pigs. *Anesthesiology* **2008**, *108* (6), 1025–1036.
- (22) Brugger, J.; Schick, M. A.; Brock, R. W.; Baumann, A.; Muellenbach, R. M.; Roewer, N.; Wunder, C. Carbon Monoxide Has Antioxidative Properties in the Liver Involving P38 MAP Kinase Pathway in a Murine Model of Systemic Inflammation. *Microcirculation* **2010**, *17* (7), 504–513.
- (23) Song, R.; Mahidhara, R. S.; Zhou, Z.; Hoffman, R. A.; Seol, D.-W.; Flavell, R. A.; Billiar, T. R.; Otterbein, L. E.; Choi, A. M. K. Carbon Monoxide Inhibits T Lymphocyte Proliferation via Caspase-Dependent Pathway. *J. Immunol.* **2004**, *172* (2), 1220–1226.
- (24) McRae, K. E.; Pudwel, J.; Peterson, N.; Smith, G. N. Inhaled carbon monoxide increases vasodilation in the microvascular circulation. *Microvasc. Res.* **2019**, *123*, 92–98.
- (25) Knauert, M.; Vangala, S.; Haslip, M.; Lee, P. J. Therapeutic Applications of Carbon Monoxide. *Oxid. Med. Cell. Longev.* **2013**, *2013*, 360815.
- (26) Motterlini, R.; Clark, J. E.; Foresti, R.; Sarathchandra, P.; Mann, B. E.; Green, C. J. Carbon Monoxide-Releasing Molecules. *Circ. Res.* **2002**, *90* (2), e17–e24.
- (27) Alberto, R.; Motterlini, R. Chemistry and Biological Activities of CO-Releasing Molecules (CORMs) and Transition Metal Complexes. *Dalton Trans.* **2007**, No. 17, 1651.
- (28) Clark, J. E.; Naughton, P.; Shurey, S.; Green, C. J.; Johnson, T. R.; Mann, B. E.; Foresti, R.; Motterlini, R. Cardioprotective Actions by a Water-Soluble Carbon Monoxide-Releasing Molecule. *Circ. Res.* **2003**, *93*(2), e2–e8.
- (29) Ulbrich, F.; Hagmann, C.; Buerkle, H.; Romao, C. C.; Schallner, N.; Goebel, U.; Biermann, J. The Carbon Monoxide Releasing Molecule ALF-186 Mediates Anti-Inflammatory and Neuroprotective Effects via the Soluble Guanylate Cyclase SS1 in Rats' Retinal Ganglion Cells after Ischemia and Reperfusion Injury. *J. Neuroinflammation* **2017**, *14* (1), 130.
- (30) Motterlini, R.; Sawle, P.; Bains, S.; Hammad, J.; Alberto, R.; Foresti, R.; Green, C. J. CORM-A1: A New Pharmacologically Active Carbon Monoxide-Releasing Molecule. *FASEB J.* **2005**, *19* (2), 1–24.

- (31) Porshneva, K.; Papiernik, D.; Psurski, M.; Łupicka-Słowik, A.; Matkowski, R.; Ekiert, M.; Nowak, M.; Jarosz, J.; Banach, J.; Milczarek, M.; Goszczyński, T. M.; Sieńczyk, M.; Wietrzyk, J. Temporal Inhibition of Mouse Mammary Gland Cancer Metastasis by CORM-A1 and DETA/NO Combination Therapy. *Theranostics* **2019**, *9* (13), 3918–3939.
- (32) Yuan, Z.; Yang, X.; Wang, B. Redox and Catalase-like Activities of Four Widely Used Carbon Monoxide Releasing Molecules (CO-RMs). *Chem. Sci.* **2021**, *12* (39), 13013–13020.
- (33) Southam, H. M.; Williamson, M. P.; Chapman, J. A.; Lyon, R. L.; Trevitt, C. R.; Henderson, P. J. F.; Poole, R. K. ‘Carbon-Monoxide-Releasing Molecule-2 (CORM-2)’ Is a Misnomer: Ruthenium Toxicity, Not CO Release, Accounts for Its Antimicrobial Effects. *Antioxidants* **2021**, *10* (6), 915.
- (34) Yuan, Z.; Yang, X.; Ye, Y.; Tripathi, R.; Wang, B. Chemical Reactivities of Two Widely Used Ruthenium-Based CO-Releasing Molecules with a Range of Biologically Important Reagents and Molecules. *Anal Chem* **2021**, *10*.
- (35) Yuan, Z.; Yang, X.; Cruz, L. K. D. L.; Wang, B. Nitro Reduction-Based Fluorescent Probes for Carbon Monoxide Require Reactivity Involving a Ruthenium Carbonyl Moiety. *Chem. Commun.* **2020**, *56* (14), 2190–2193.
- (36) Faizan, M.; Muhammad, N.; Niazi, K. U. K.; Hu, Y.; Wang, Y.; Wu, Y.; Sun, H.; Liu, R.; Dong, W.; Zhang, W.; Gao, Z. CO-Releasing Materials: An Emphasis on Therapeutic Implications, as Release and Subsequent Cytotoxicity Are the Part of Therapy. *Materials* **2019**, *12* (10), 1643.
- (37) Ji, X.; Pan, Z.; Li, C.; Kang, T.; De La Cruz, L. K. C.; Yang, L.; Yuan, Z.; Ke, B.; Wang, B. Esterase-Sensitive and PH-Controlled Carbon Monoxide Prodrugs for Treating Systemic Inflammation. *J. Med. Chem.* **2019**, *62* (6), 3163–3168.
- (38) Stamellou, E.; Storz, D.; Botov, S.; Ntasis, E.; Wedel, J.; Sollazzo, S.; Kramer, B. K.; Son, W. V.; Seelen, M.; Schmalz, H. G.; Schmidt, A.; Hafner, M.; Yard, B. A. Different design of enzyme-triggered CO-releasing molecules (ET-CORMs) reveals quantitative differences in biological activities in terms of toxicity and inflammation. *Redox. Bio.* **2014**, *2*, 739–748.
- (39) Zhang, D.; Krause, B. M.; Schmalz, H.-G.; Wohlfart, P.; Yard, B. A.; Schubert, R. ET-CORM Mediated Vasorelaxation of Small Mesenteric Arteries: Involvement of Kv7 Potassium Channels. *Front. Pharmacol.* **2021**, *12*.
- (40) Rimmer, R. D.; Richter, H.; Ford, P. C. A Photochemical Precursor for Carbon Monoxide Release in Aerated Aqueous Media. *Inorg. Chem.* **2010**, *49* (3), 1180–1185.
- (41) Popova, M.; Lazarus, L. S.; Ayad, S.; Benninghoff, A. D.; Berreau, L. M. Visible-Light-Activated Quinolone Carbon-Monoxide-Releasing Molecule: Prodrug and Albumin-Assisted Delivery Enables Anticancer and Potent Anti-Inflammatory Effects. *J. Am. Chem. Soc.* **2018**, *140* (30), 9721–9729.
- (42) Wang, D.; Viennois, E.; Ji, K.; Damera, K.; Draganov, A.; Zheng, Y.; Dai, C.; Merlin, D.; Wang, B. A Click-and-Release Approach to CO Prodrugs. *Chem Commun* **2014**, *50* (100), 15890–15893.
- (43) Ji, X.; Wang, B. Strategies toward Organic Carbon Monoxide Prodrugs. *Acc. Chem. Res.* **2018**, *51* (6), 1377–1385.
- (44) Ji, X.; Zhou, C.; Ji, K.; Aghoghovbia, R.; Pan, Z.; Chittavong, V.; Ke, B.; Wang, B. Click and Release: A Chemical Strategy toward Developing Gasotransmitter Prodrugs by Using an Intramolecular Diels–Alder Reaction. *Angew. Chem.* **2016**, *55*(51), 15846–15851.

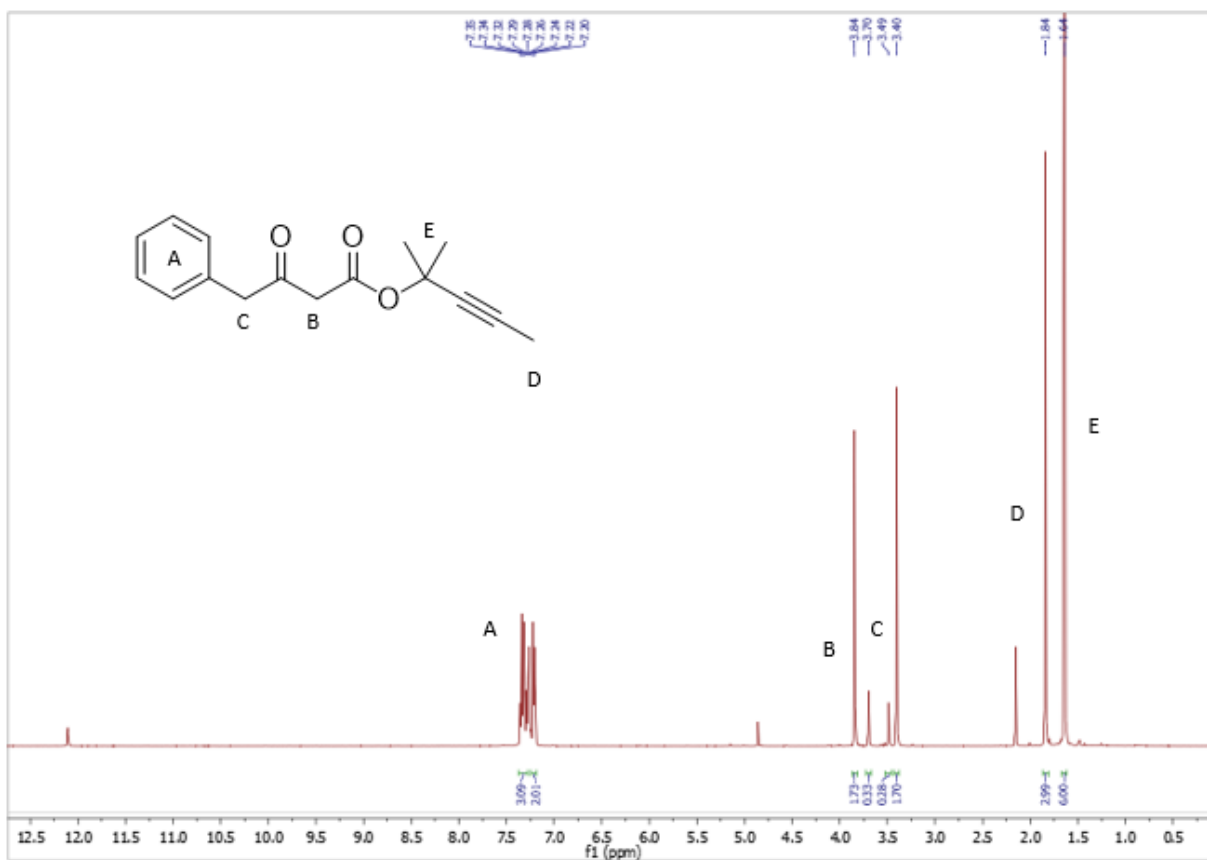
- (45) Chittavong, V. THESIS; Synthesis Of Novel Organic Carbon Monoxide Prodrugs With Tunable Release For Biological Applications. **2017**, 154.
- (46) Pan, Z.; Chittavong, V.; Li, W.; Zhang, J.; Ji, K.; Zhu, M.; Ji, X.; Wang, B. Organic CO-Prodrugs: Structure CO-Release Rate Relationship Studies. *Chem. Weinh. Bergstr. Ger.* **2017**, 23 (41), 9838–9845.

5 APPENDIX

NMR Spectra

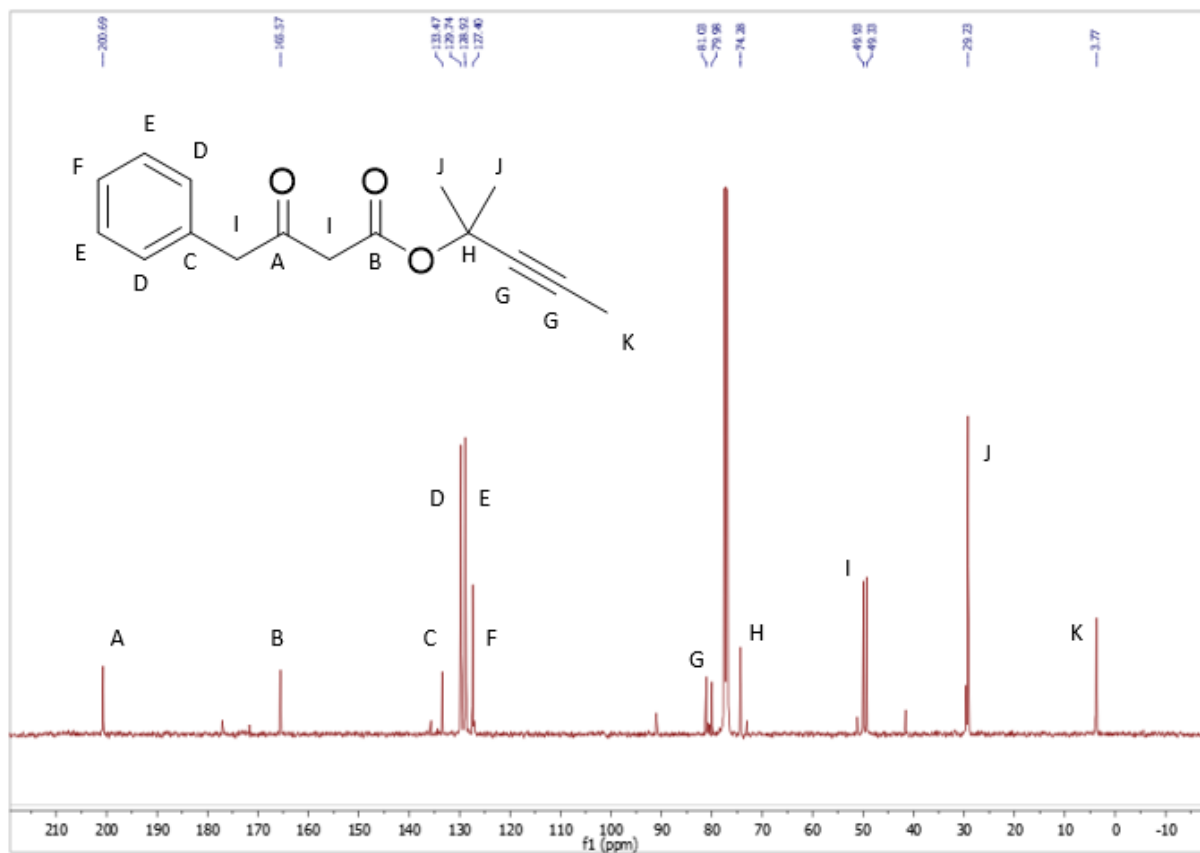


^1H NMR spectrum of 2,2-Dimethyl-5-(2-phenylacetyl)-1,3-dioxane-4,6-dione (**1a**) in CDCl_3 .

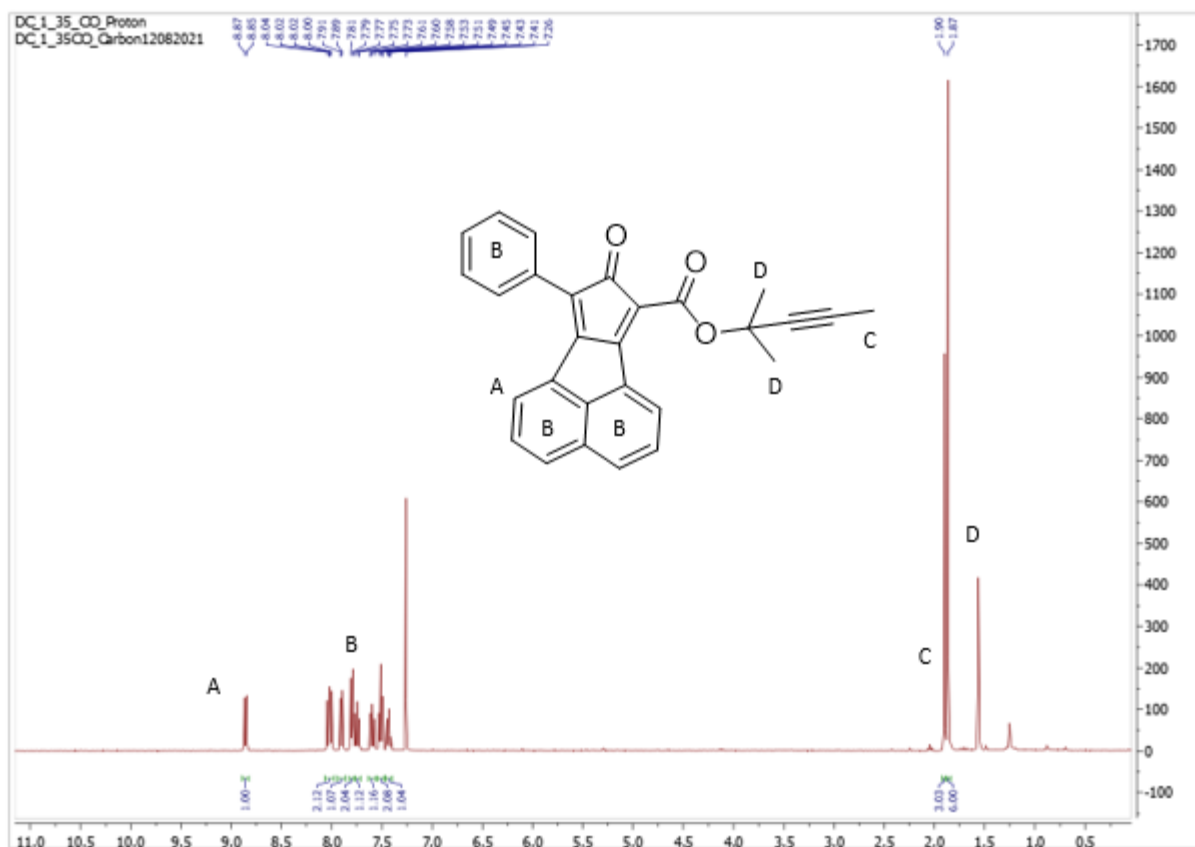


^1H NMR spectrum of 2-Methylpent-3-yn-2-yl 3-oxo-4-phenylbutanoate (**2a**) in CDCl₃.

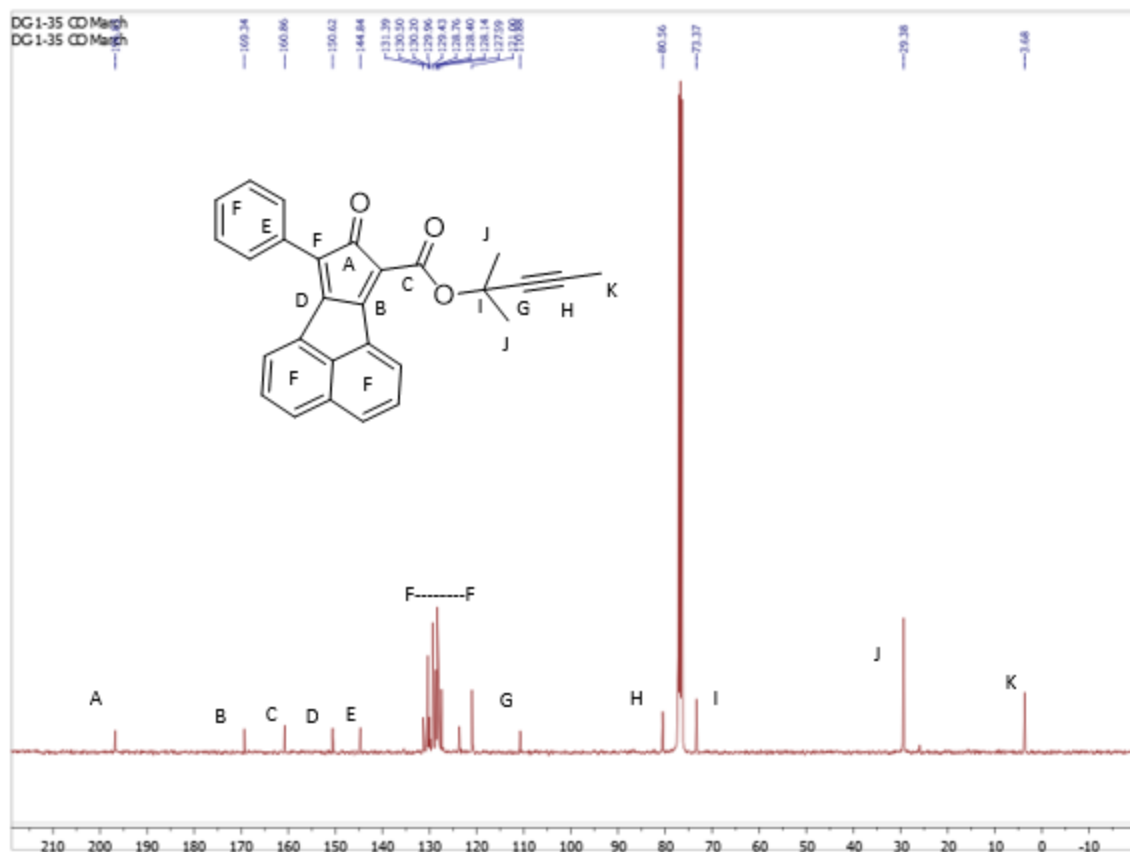
Small peaks between 3 and 4 ppm are the enol form.



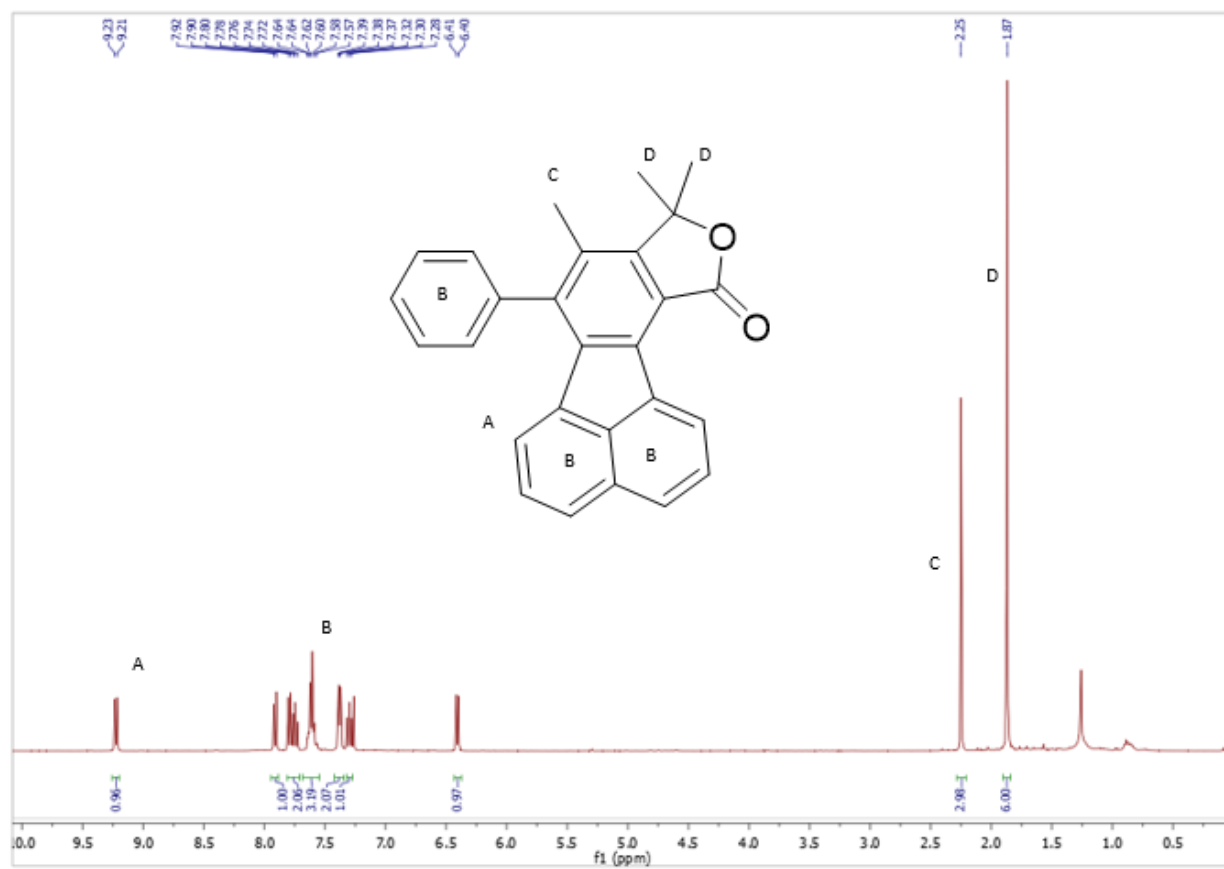
^{13}C NMR spectrum of 2-Methylpent-3-yn-2-yl 3-oxo-4-phenylbutanoate (**2a**) in CDCl_3 .



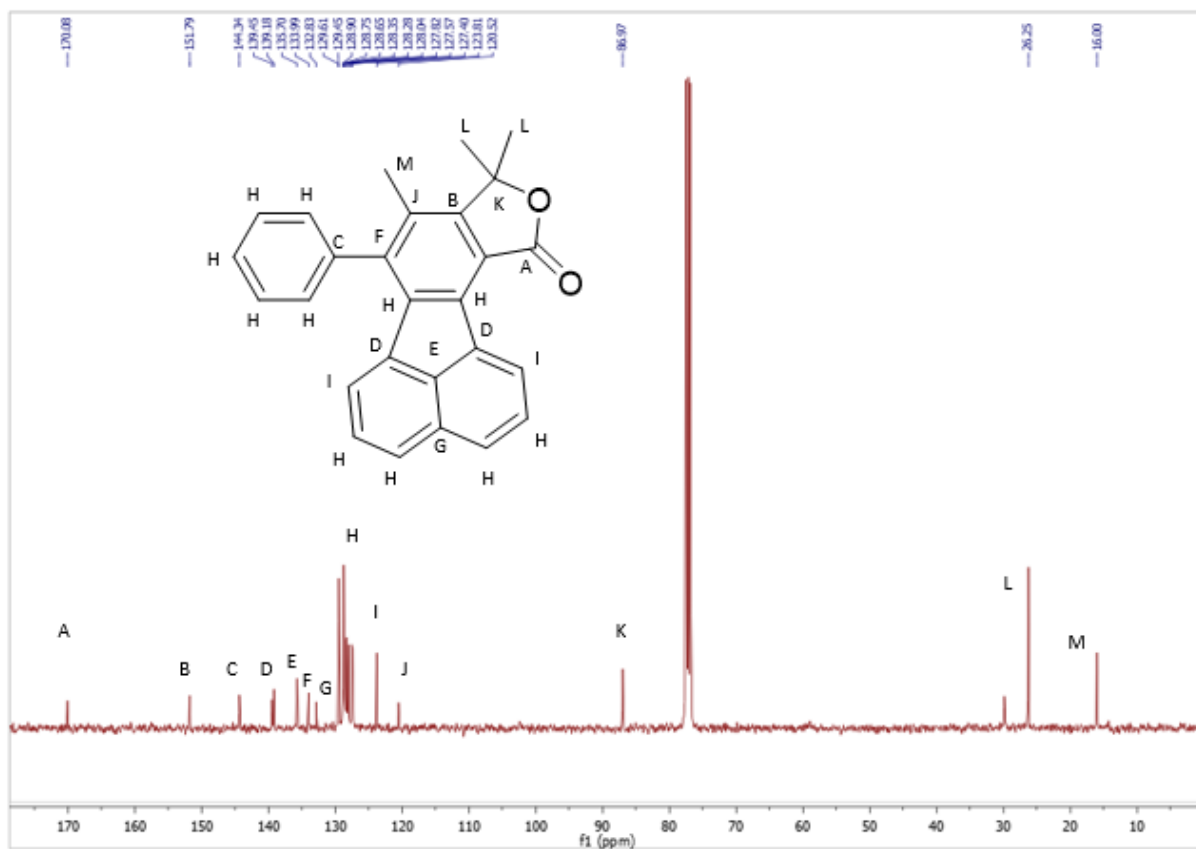
^1H NMR spectrum of **BW-CO-138 (3a)** in CDCl₃.



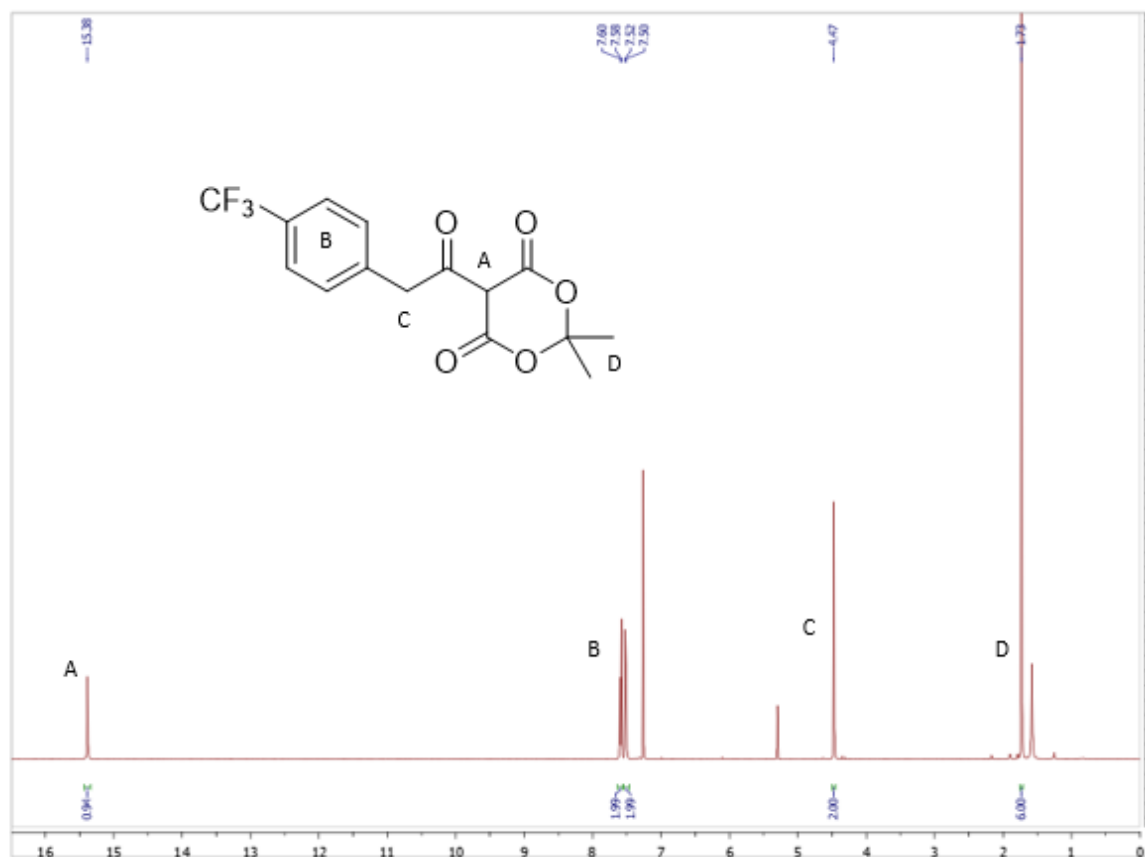
^{13}C NMR spectrum of **BW-CO-138 (3a)** in CDCl_3 .



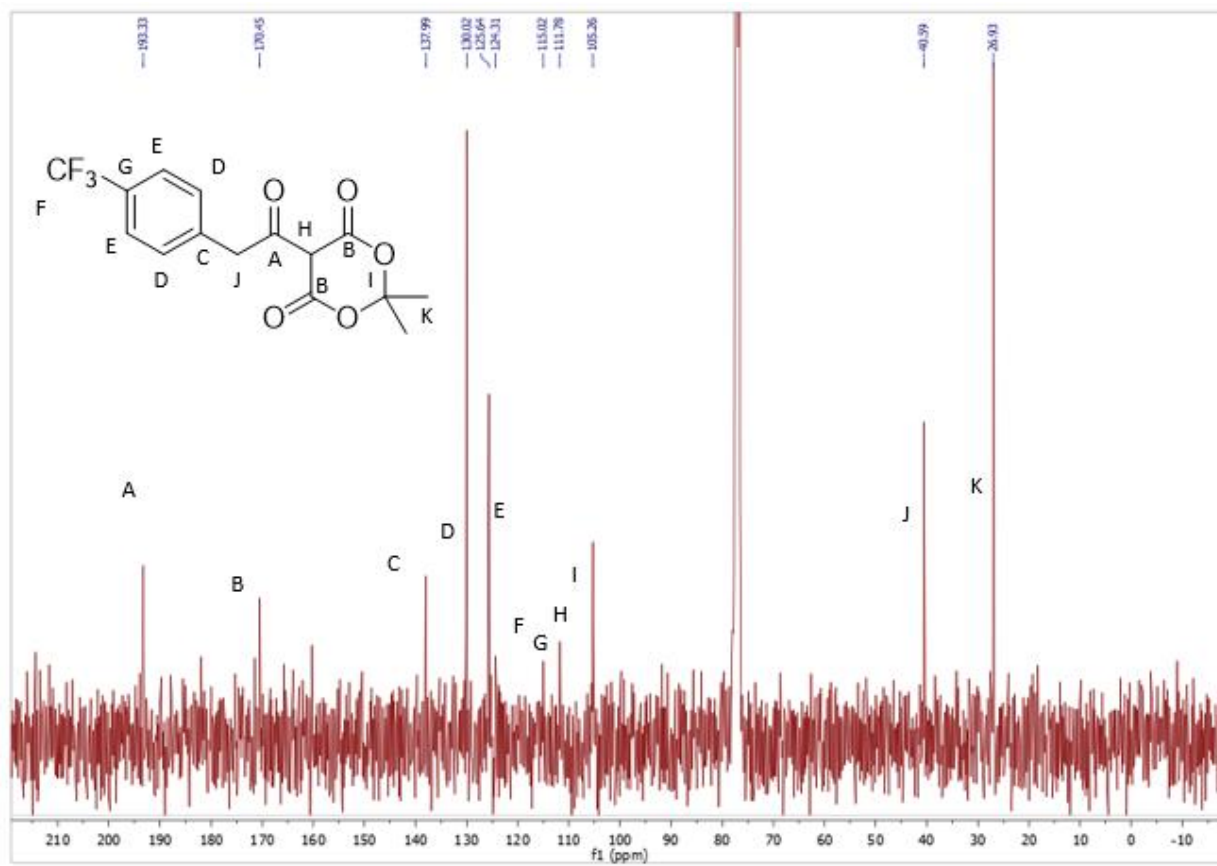
^1H NMR spectrum of **BW-CP-138 (4a)** in CDCl₃.



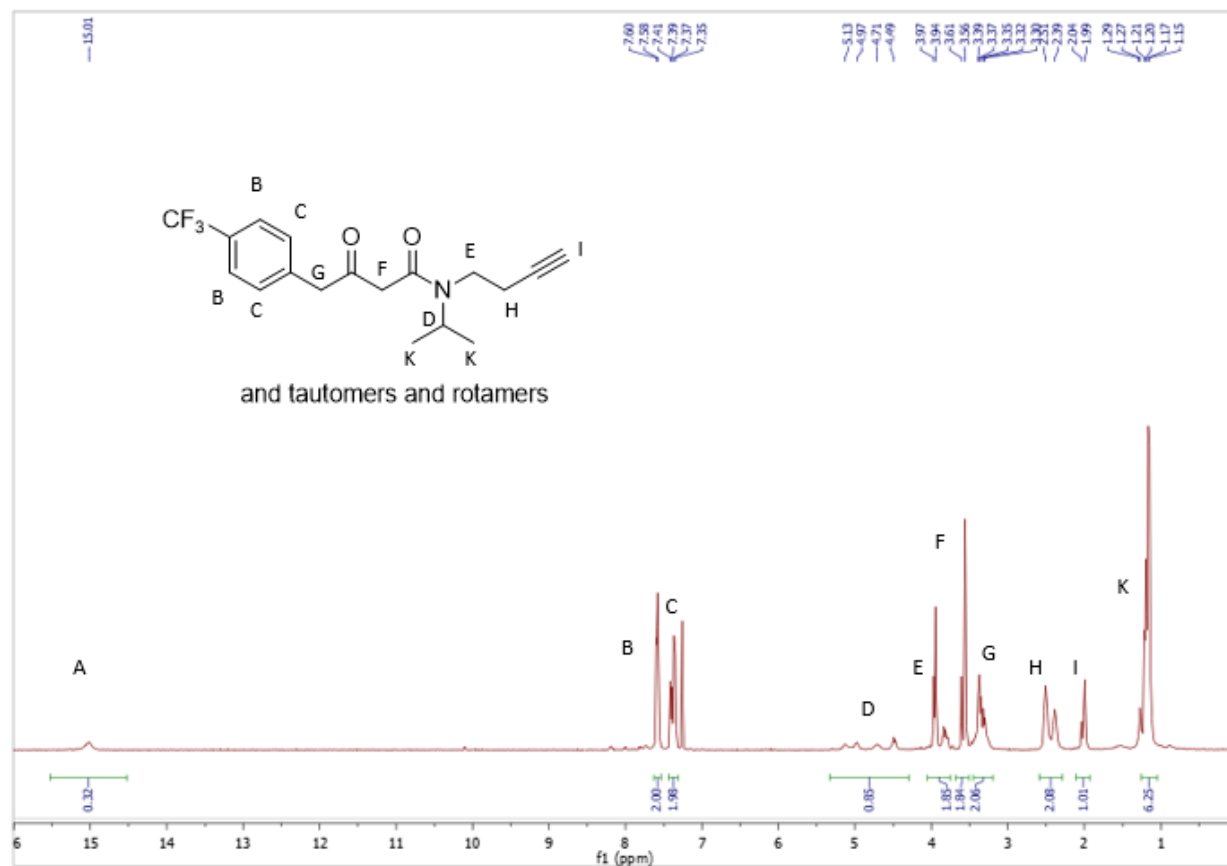
¹³C NMR spectrum of **BW-CP-138 (4a)** in CDCl₃.



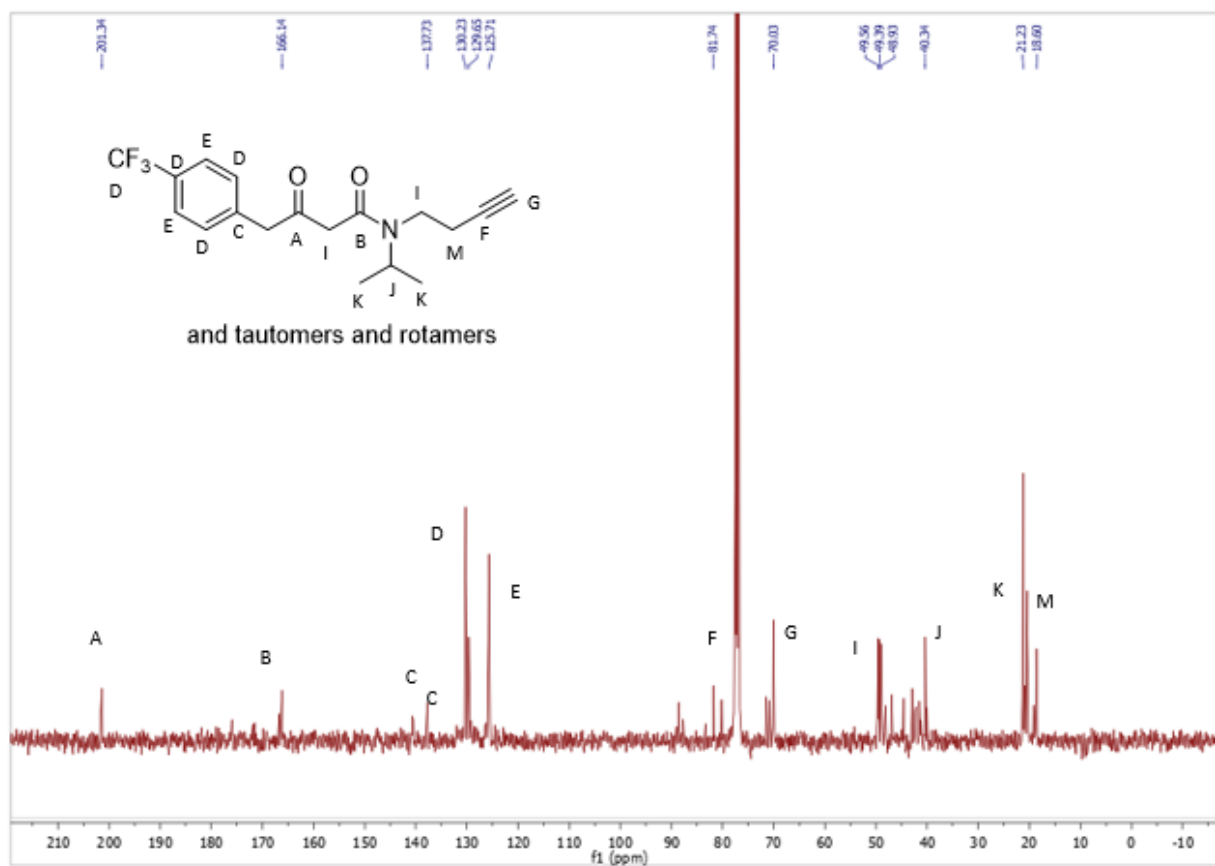
¹H NMR spectrum of 2,2-Dimethyl-5-(2-(4-(trifluoromethyl)phenyl)acetyl)-1,3-dioxane-4,6-dione (**1b**) in CDCl₃.



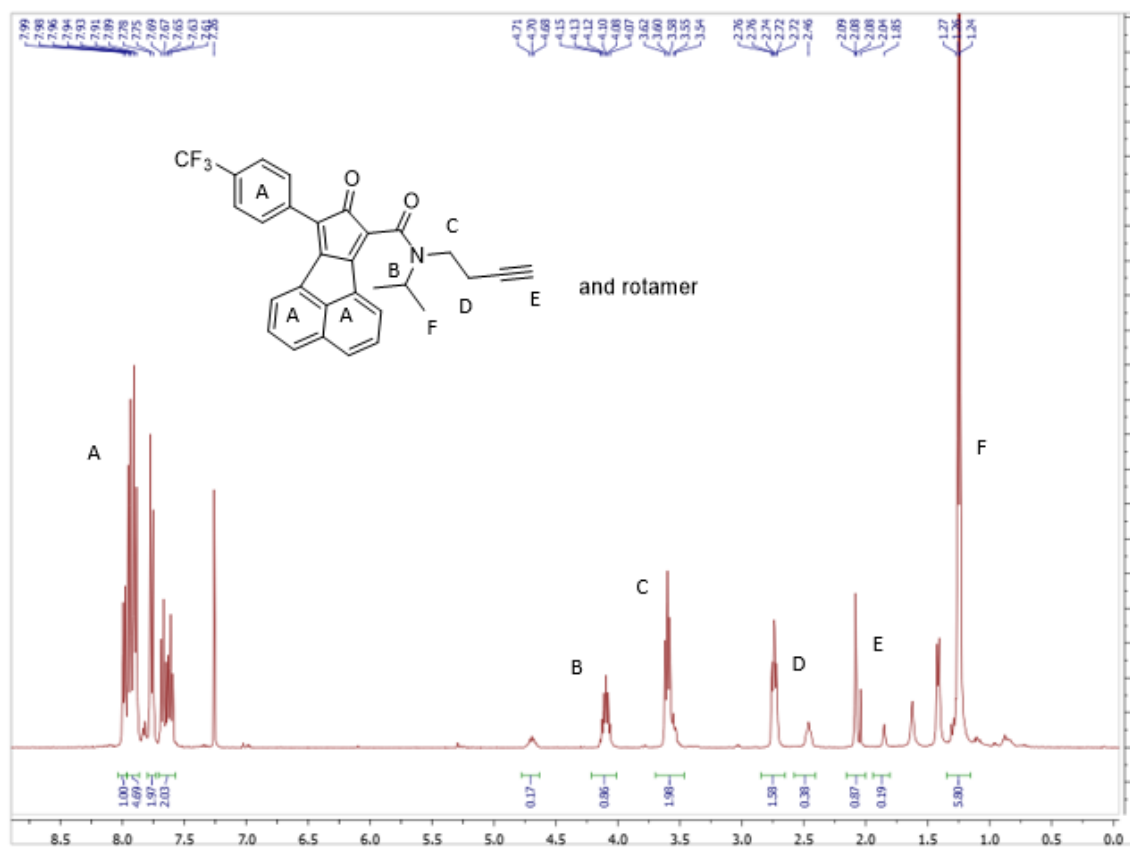
¹³C NMR spectrum of 2,2-Dimethyl-5-(2-(4-(trifluoromethyl)phenyl)acetyl)-1,3-dioxane-4,6-dione (**1b**) in CDCl₃.



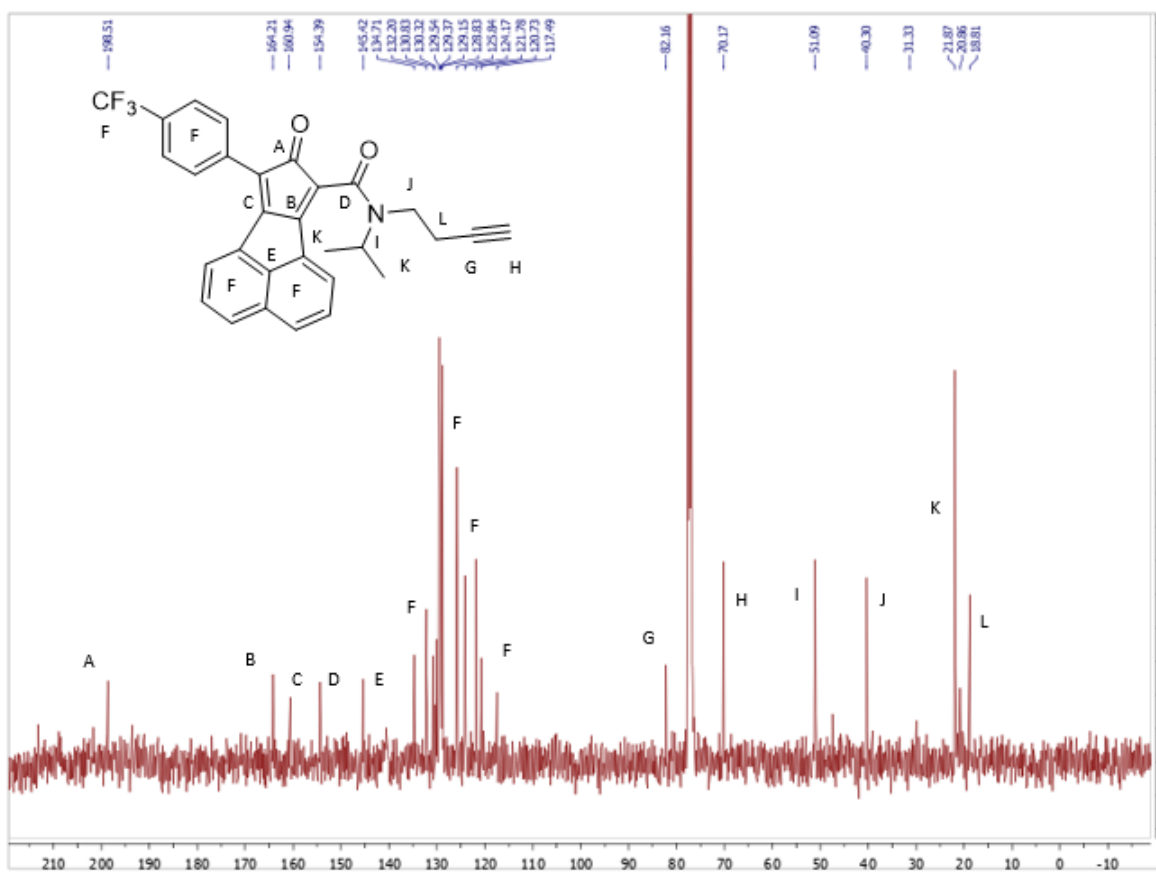
¹H NMR spectrum of *N*-(But-3-yn-1-yl)-*N*-isopropyl-3-oxo-4-(4-(trifluoromethyl)phenyl)butanamide (**2b**) in CDCl₃.



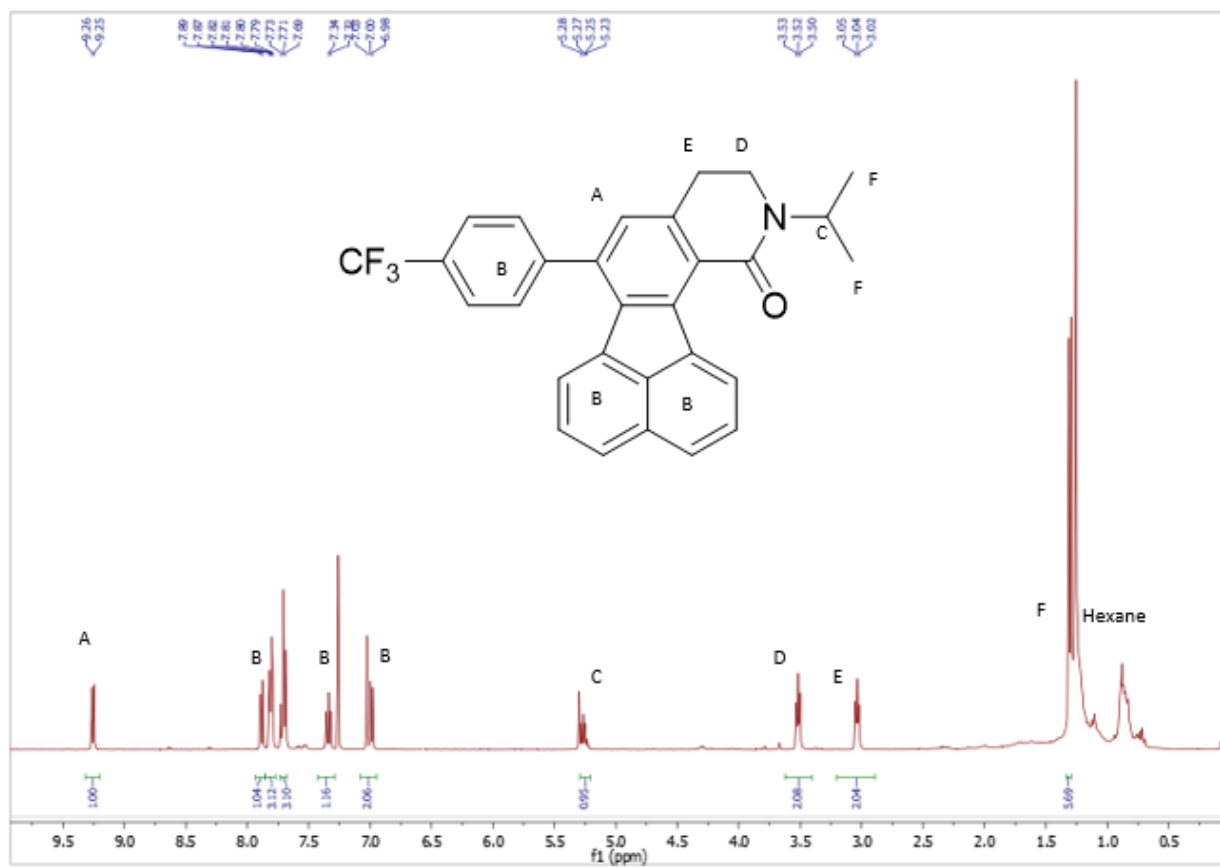
¹³C NMR spectrum of *N*-(But-3-yn-1-yl)-*N*-isopropyl-3-oxo-4-(4-(trifluoromethyl)phenyl)butanamide (**2b**) in CDCl₃.



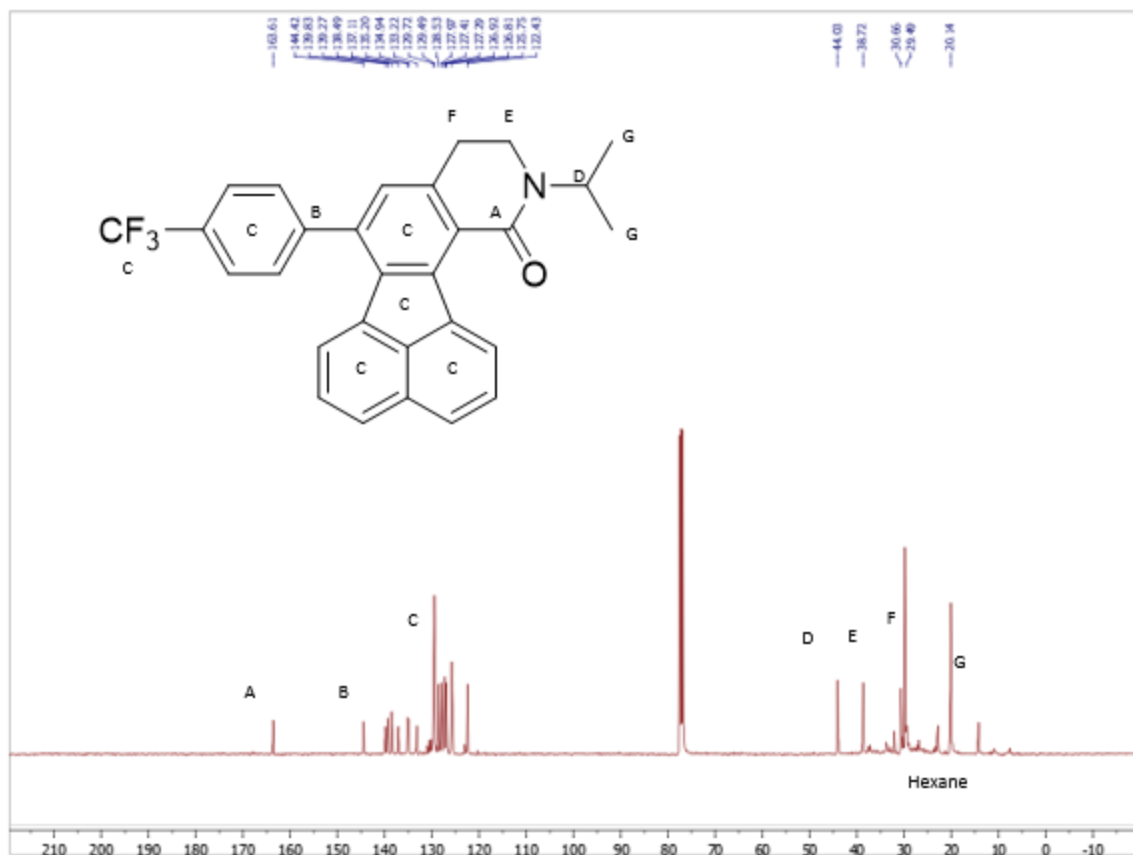
¹H NMR spectrum of **BW-CO-139 (3b)** in CDCl₃.



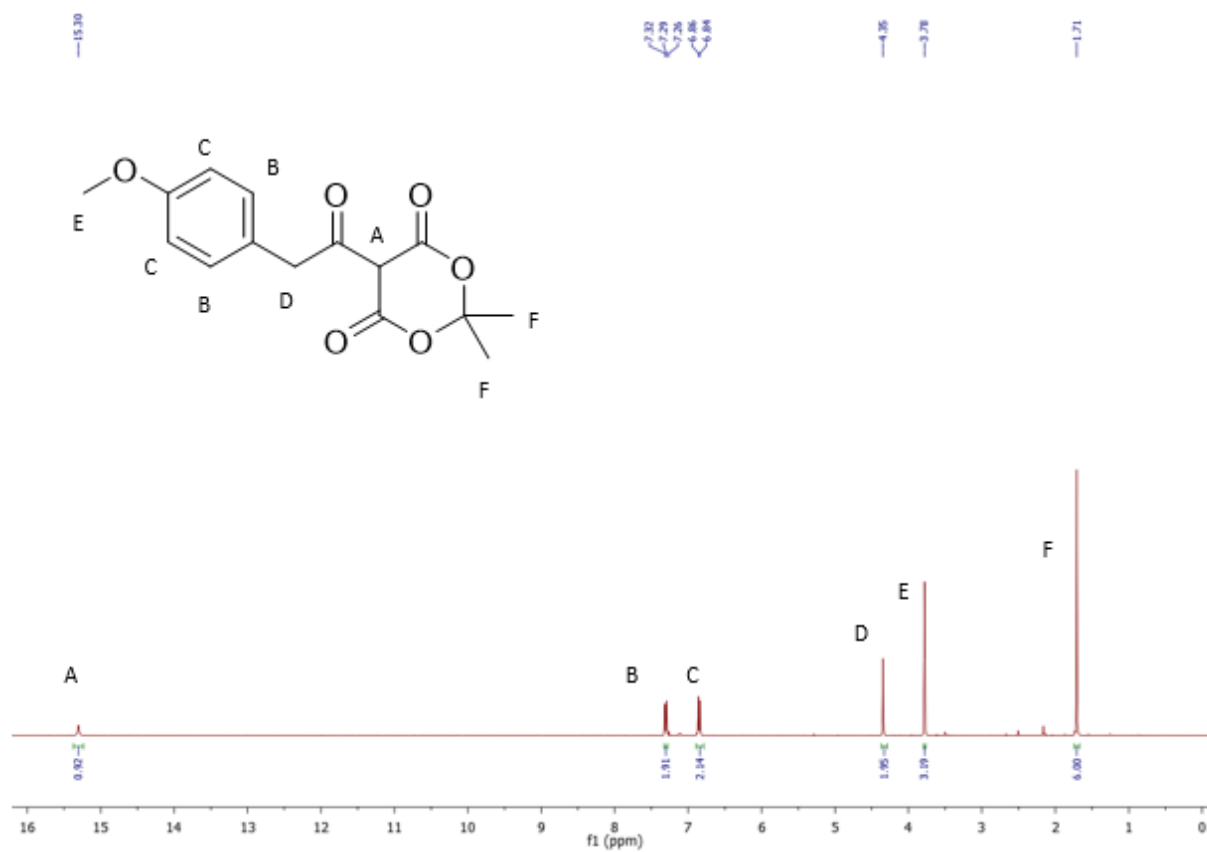
^{13}C NMR spectrum of **BW-CO-139 (3b)** in CDCl_3 .



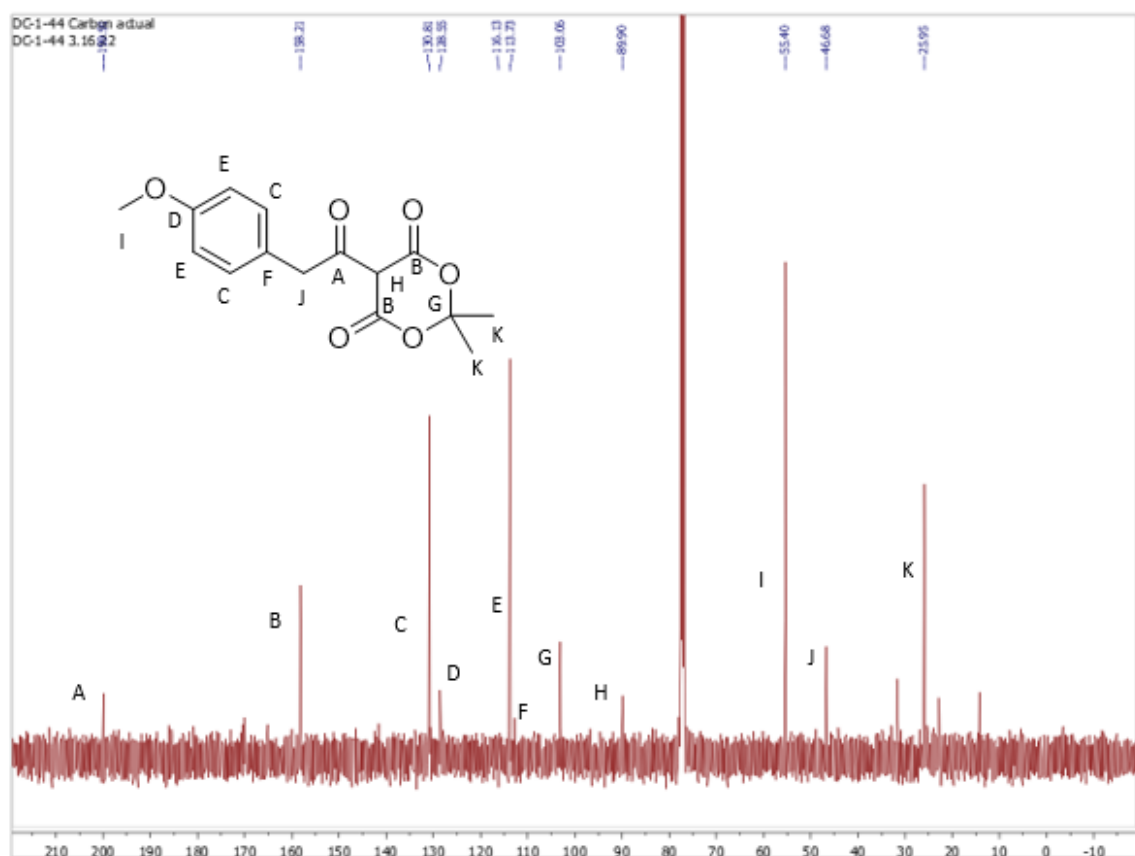
¹H NMR spectrum of **BW-CP-139 (4b)** in CDCl₃.



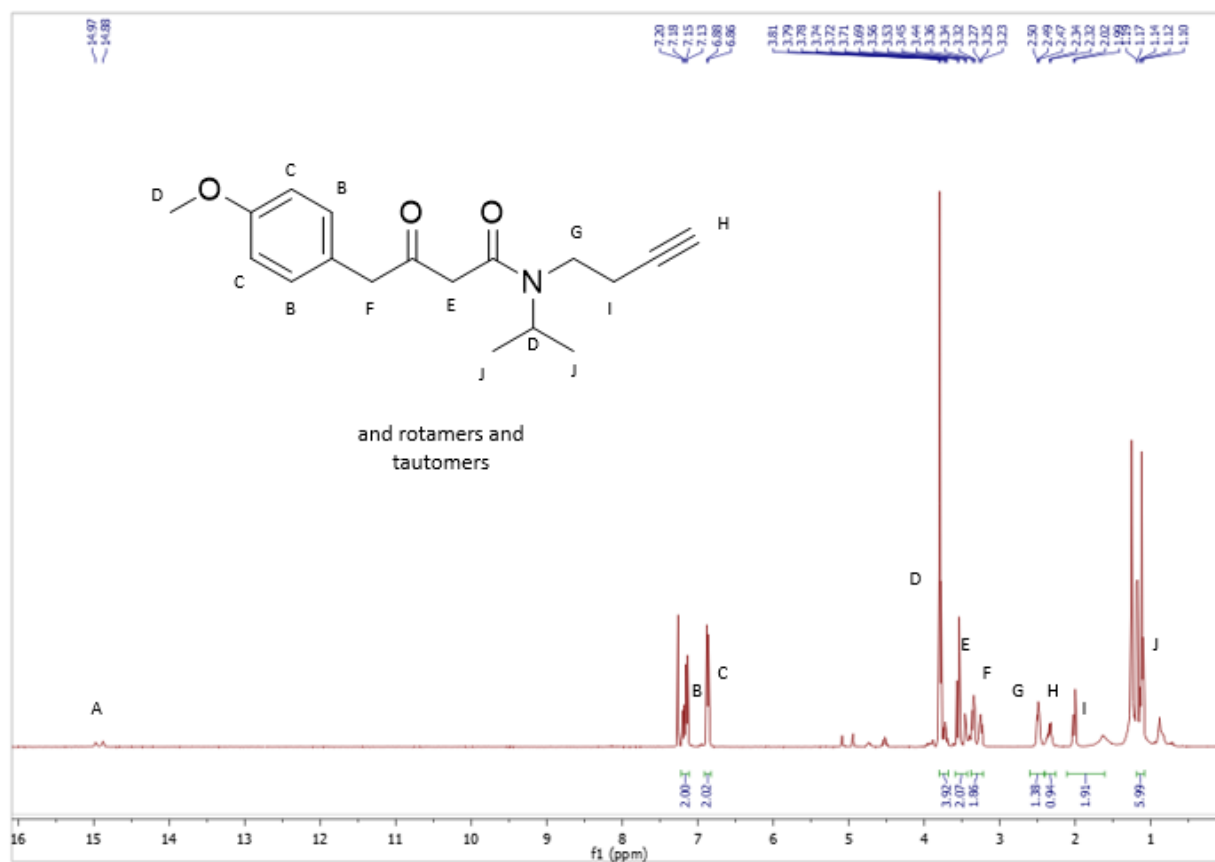
¹³C NMR spectrum of **BW-CP-139 (4b)** in CDCl₃. Hexane contamination is present.



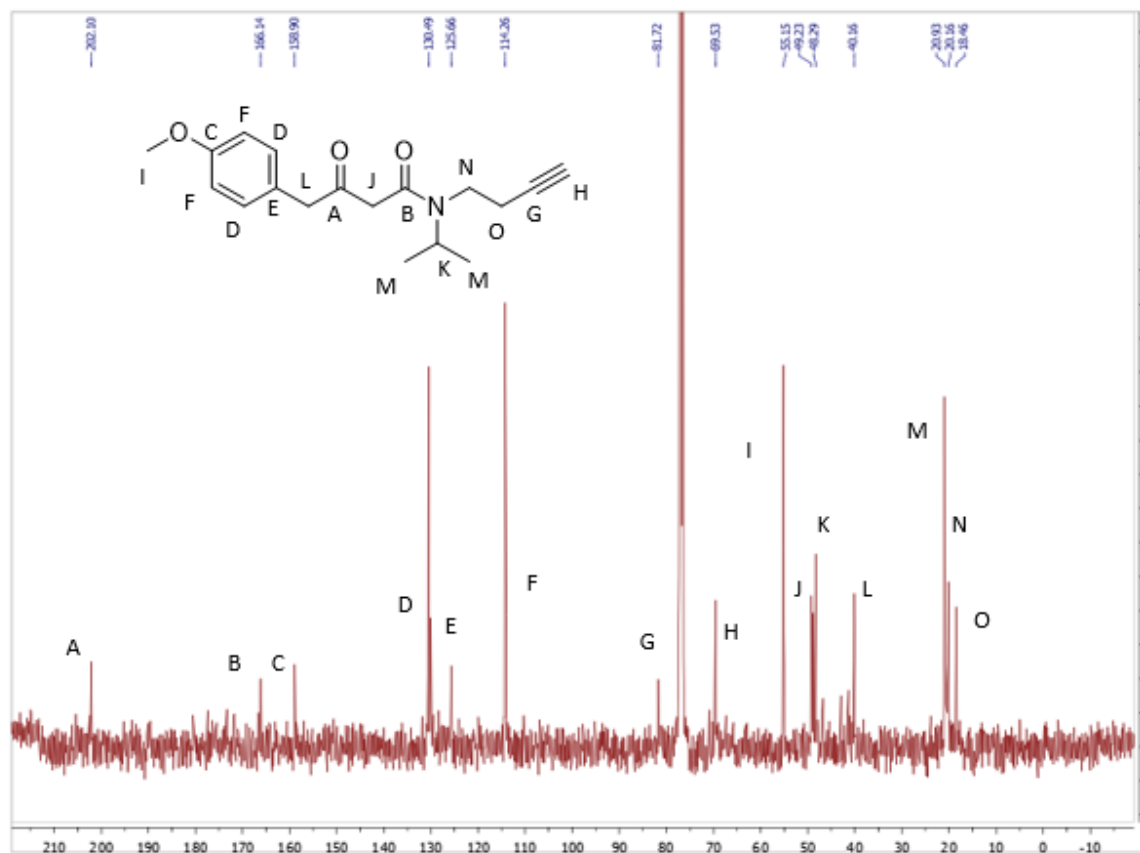
¹H NMR Spectrum of 5-(2-(4-Methoxyphenyl)acetyl)-2,2-dimethyl-1,3-dioxane-4,6-dione in CDCl₃.



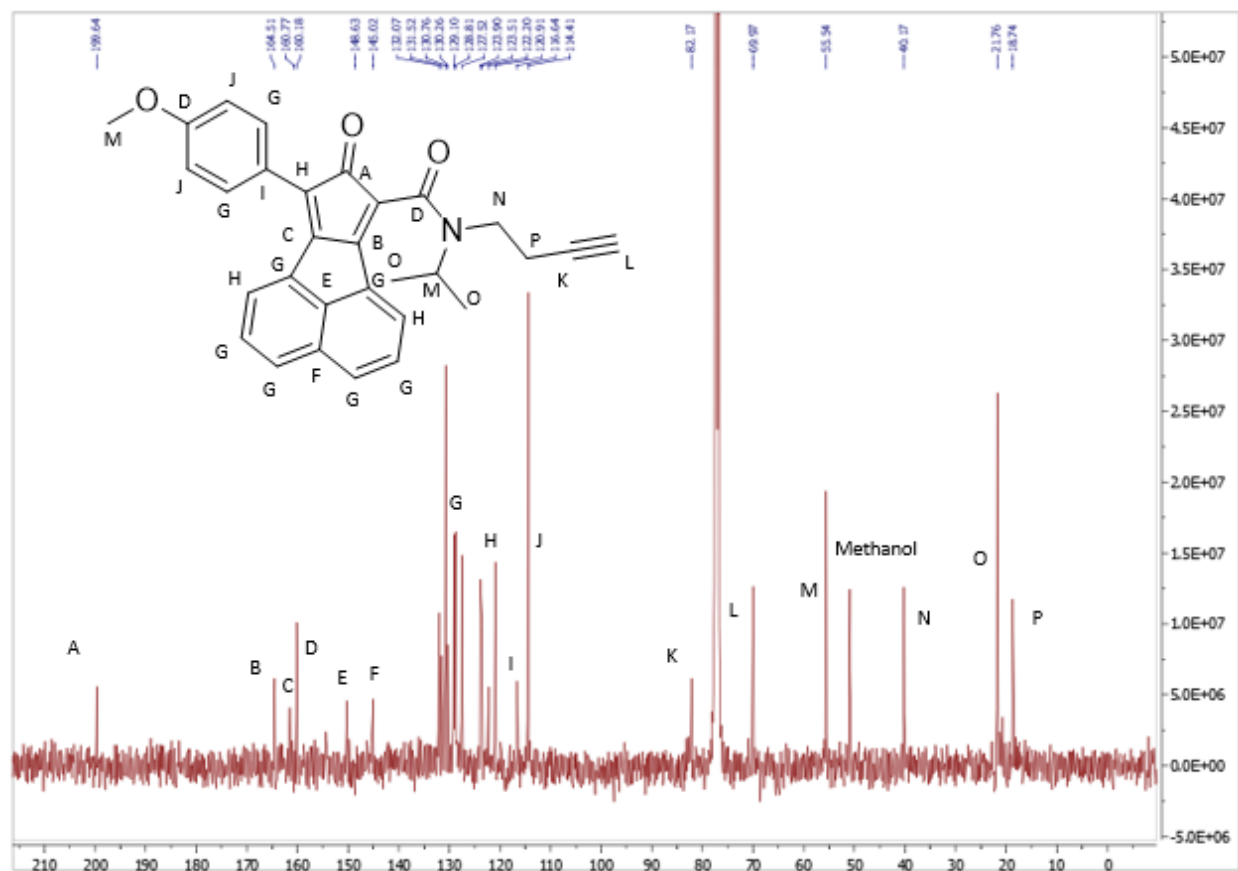
^{13}C NMR Spectrum of 5-(2-(4-Methoxyphenyl)acetyl)-2,2-dimethyl-1,3-dioxane-4,6-dione in CDCl_3 .



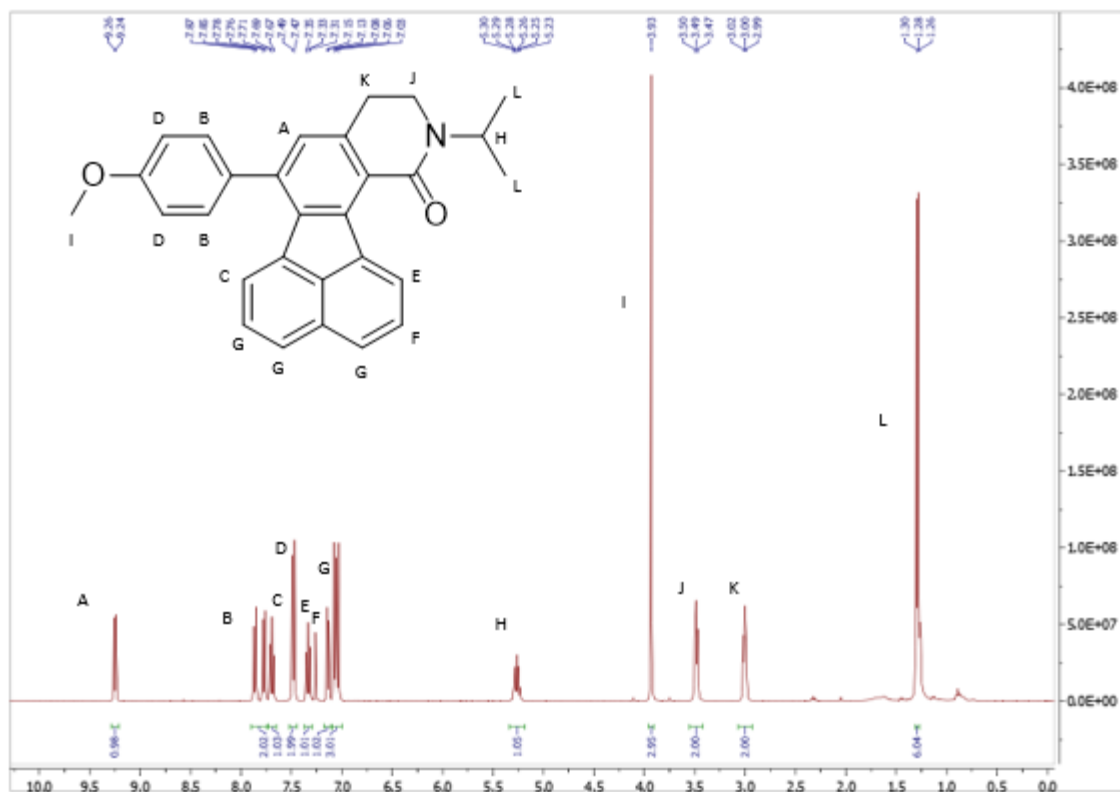
¹H NMR spectrum of *N*-(But-3-yn-1-yl)-*N*-isopropyl-4-(4-methoxyphenyl)-3-oxobutanamide in CDCl₃.



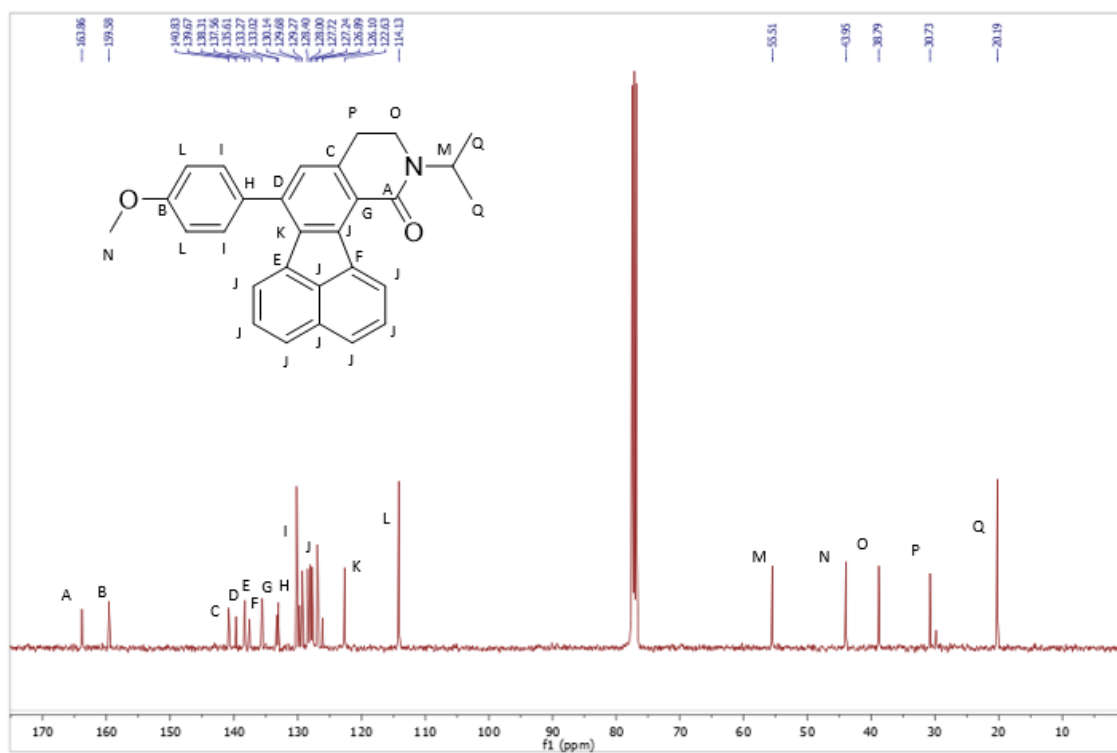
¹³C NMR spectrum of *N*-(But-3-yn-1-yl)-*N*-isopropyl-4-(4-methoxyphenyl)-3-oxobutanamide in CDCl₃.



^{13}C NMR Spectrum of **BW-CO-140, 3c**, in CDCl_3 .



^1H NMR Spectrum of **BW-CP-140, 4c**, in CDCl_3 .



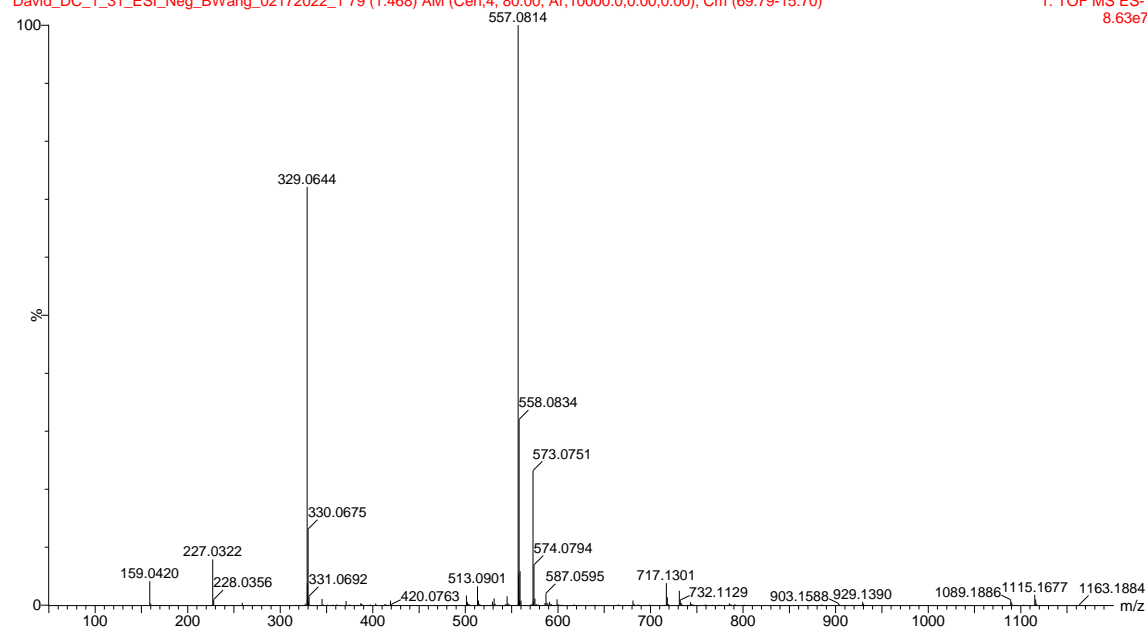
¹³C NMR Spectrum of **BW-CP-140, 4c**, in CDCl₃.

Mass Spectra

75%MeOH+0.1%HCOOH, 100uL/min, 2x50mm BEH

David_DC_1_31_ESI_Neg_BWang_02172022_1 79 (1.468) AM (Cen,4, 80.00, Ar,10000.0,0.00,0.00); Cm (69:79-15:70)

1: TOF MS ES-
8.63e7

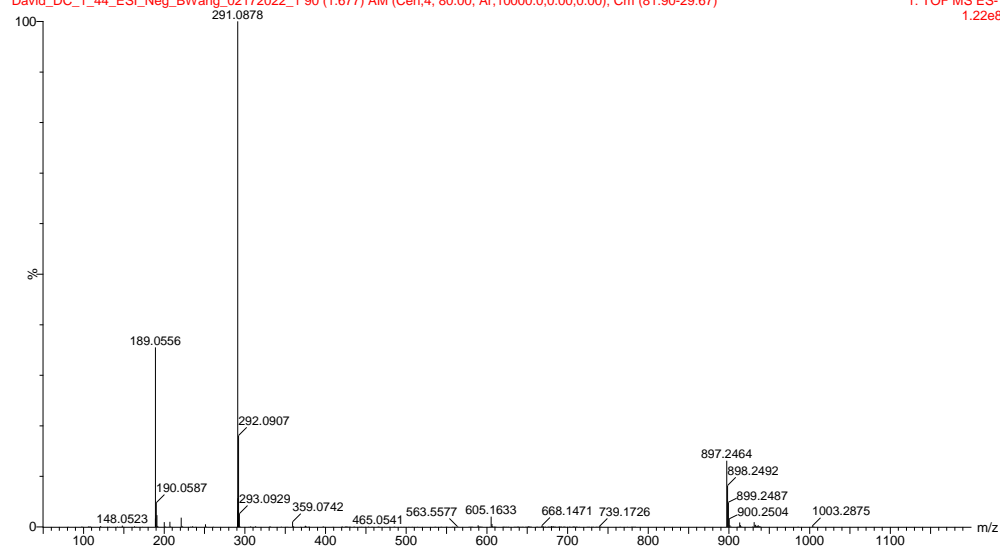


Mass Spectrum of **1b**, 2,2-dimethyl-5-(2-(4-(trifluoromethyl)phenyl)acetyl)-1,3-dioxane-4,6-dione

75%MeOH+0.1%HCOOH, 100uL/min, 2x50mm BEH

David_DC_1_44_ESI_Neg_BWang_02172022_1 90 (1.677) AM (Cen,4, 80.00, Ar,10000.0,0.00,0.00); Cm (81:90-29:67)

1: TOF MS ES-
1.22e8

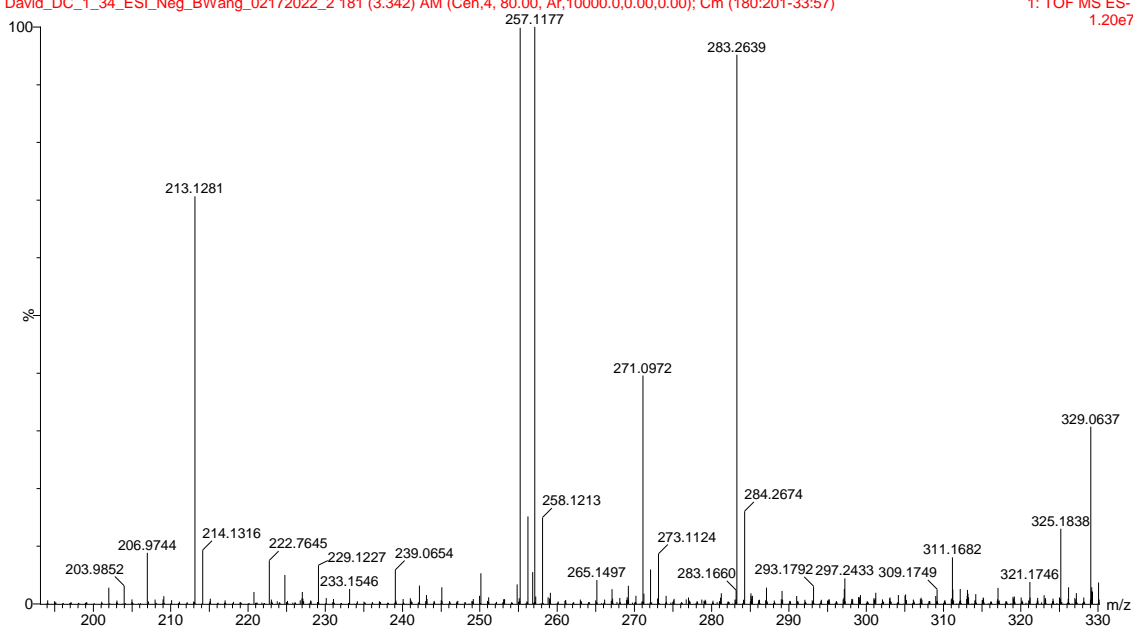


Mass Spectrum of **1c**, 5-(2-(4-methoxyphenyl)acetyl)-2,2-dimethyl-1,3-dioxane-4,6-dione

75%MeOH+0.1%HCOOH, 100uL/min, 2x50mm BEH

David_DC_1_34_ESI_Neg_BWang_02172022_2 181 (3.342) AM (Cen,4, 80.00, Ar,10000.0,0.00,0.00); Cm (180:201-33:57)

1: TOF MS ES-
1.20e7

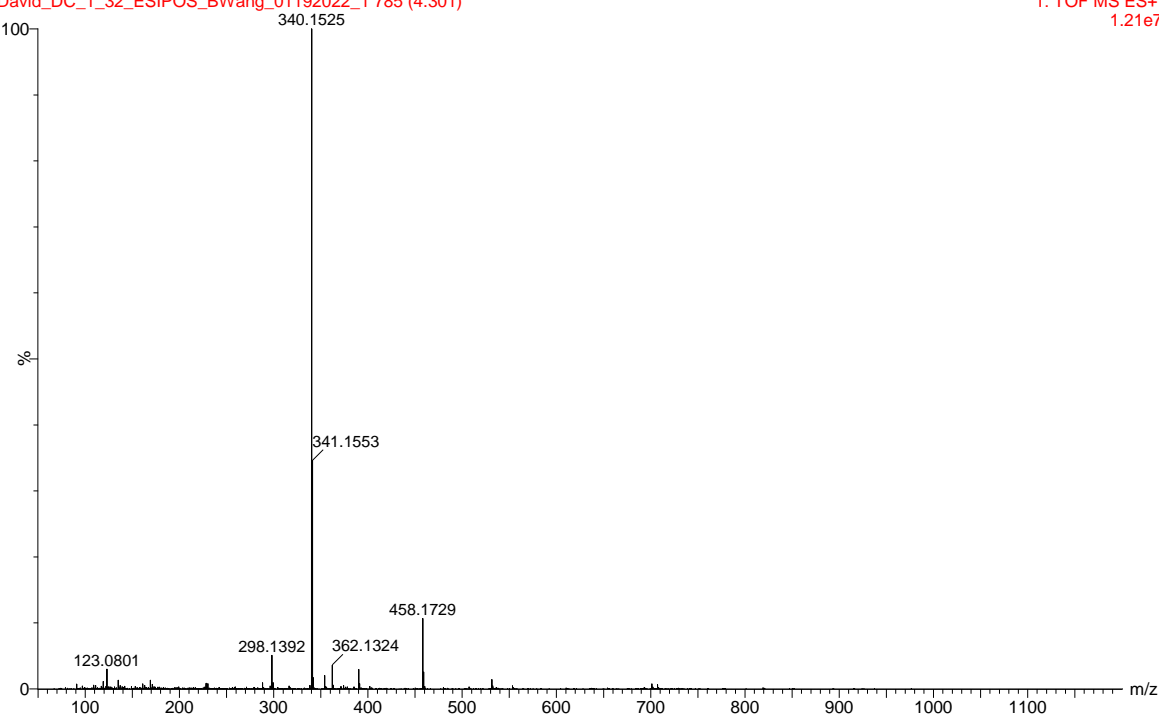


Mass Spectrum of **2a**, 2-methylpent-3-yn-2-yl 3-oxo-4-phenylbutanoate

in 75%MeOH+0.1%HCOOH, 100uL per min in 75%MeOH+0.1%HCOOH

David_DC_1_32_ESIPOS_BWang_01192022_1 785 (4.301)

1: TOF MS ES+
1.21e7

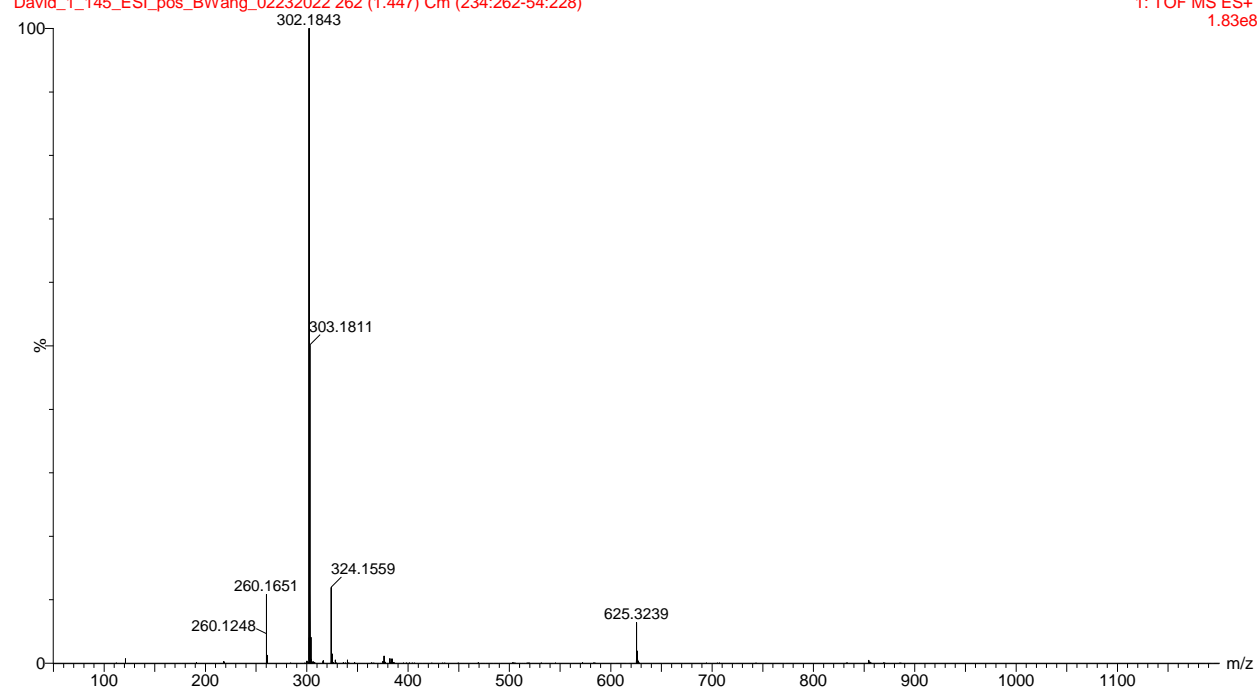


Mass Spectrum of **2b**, *N*-(but-3-yn-1-yl)-*N*-isopropyl-3-oxo-4-(4-(trifluoromethyl)phenyl)butanamide

75%MeOH+0.1%HCOOH, 100uL/min,

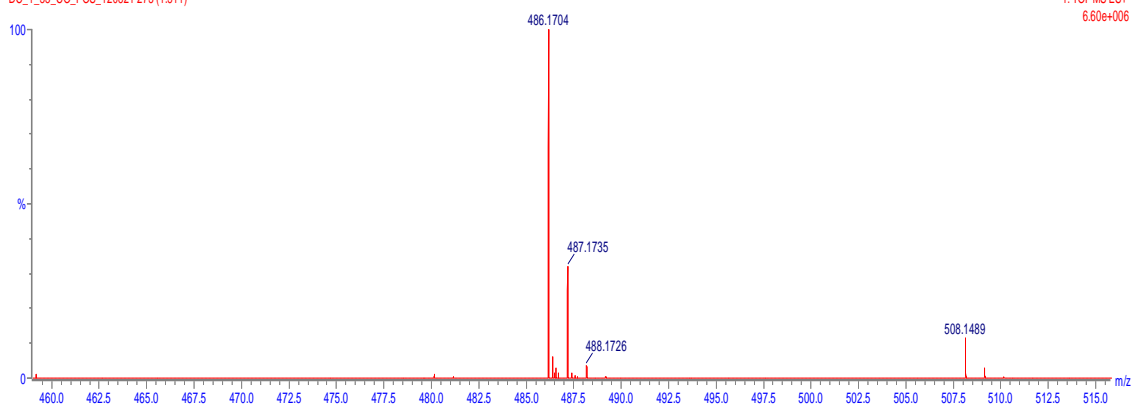
David_1_145_ESI_pos_BWang_02232022 262 (1.447) Cm (234:262-54:228)

1: TOF MS ES+
1.83e8



Mass Spectrum of **2c**, *N*-(but-3-yn-1-yl)-*N*-isopropyl-4-(4-methoxyphenyl)-3-oxobutanamide

NO COLUMN no quad profile 100uL/min 50%MeOH+0.1%FA
DC_1_33_CO_POS_120821 273 (1.511)

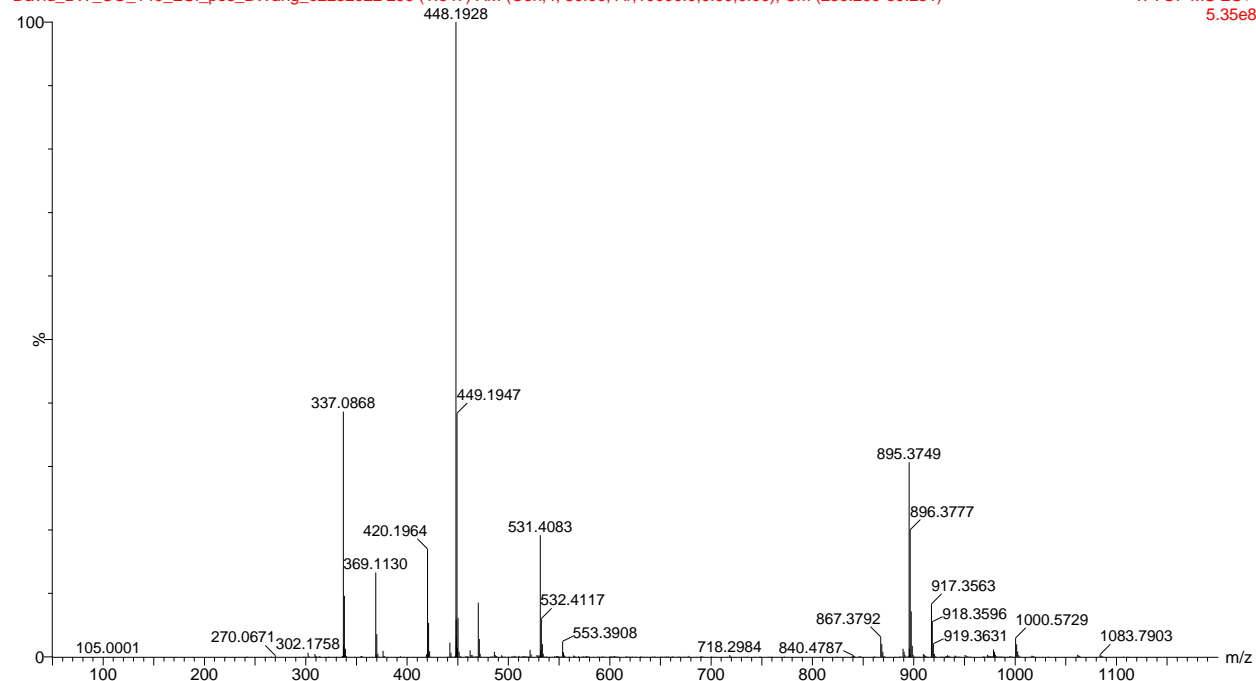


1: TOF MS ES+
6.60e+006

Mass Spectrum of **3b**, *N*-(but-3-yn-1-yl)-*N*-isopropyl-8-oxo-9-(4-(trifluoromethyl)phenyl)-8H-cyclopenta[*a*]acenaphthylene-7-carboxamide, **BW-CO-139**:

75%MeOH+0.1%HCOOH, 100uL/min,

David_BW_CO_140_ESI_pos_BWang_02232022 299 (1.647) AM (Cen,4, 80.00, Ar,10000.0,0.00,0.00); Cm (259:299-59:251)

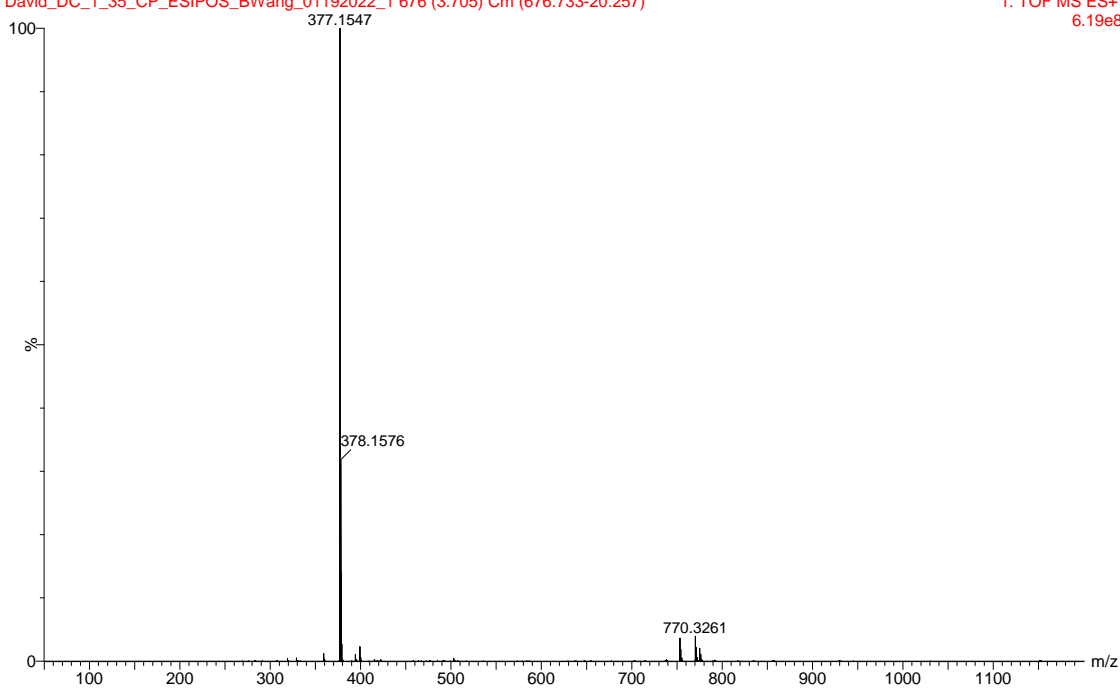


1: TOF MS ES+
5.35e8

Mass Spectrum of **3c**, *N*-(but-3-yn-1-yl)-*N*-isopropyl-9-(4-methoxyphenyl)-8-oxo-8H-cyclopenta[*a*]acenaphthylene-7-carboxamide, **BW-CO-140**:

in 75%MeOH+0.1%HCOOH, 100uL per min in 75%MeOH+0.1%HCOOH
David_DC_1_35_CP_ESIPOS_BWang_01192022_1 676 (3.705) Cm (676:733-20:257)

1: TOF MS ES+
6.19e8

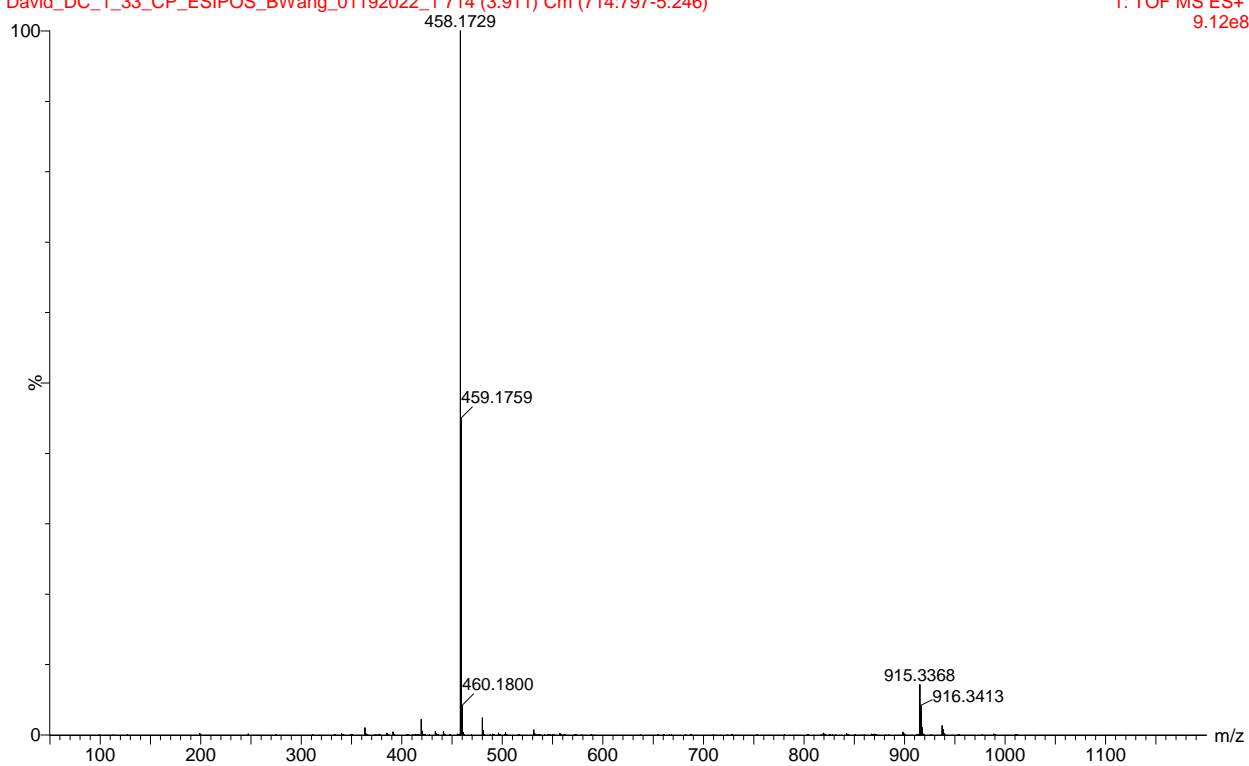


Mass Spectrum of **4a**, 3,3,4-trimethyl-5-phenylfluorantheno[7,8-c]furan-1(3H)-one, **BW-CP-**

138:

in 75%MeOH+0.1%HCOOH, 100uL per min in 75%MeOH+0.1%HCOOH
David_DC_1_33_CP_ESIPOS_BWang_01192022_1 714 (3.911) Cm (714:797-5:246)

1: TOF MS ES+
9.12e8

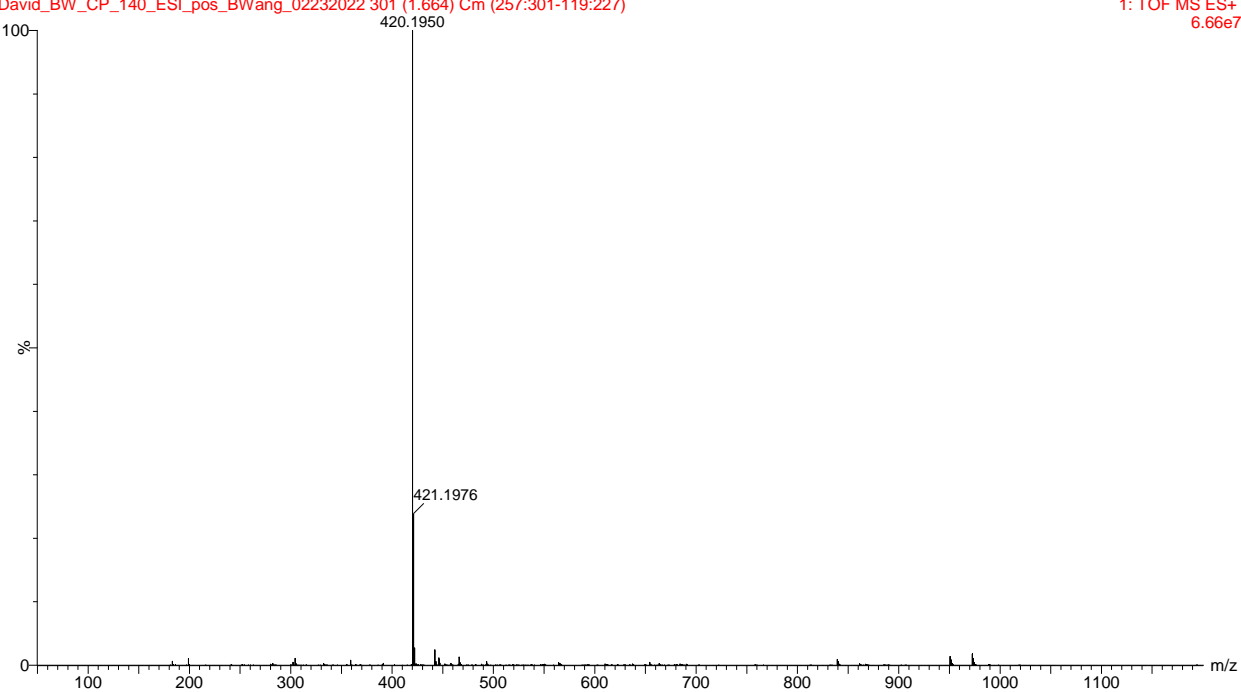


Mass Spectrum of **4b**, 2-isopropyl-6-(4-(trifluoromethyl)phenyl)-3,4-dihydroacenaphtho[1,2-h]isoquinolin-1(2H)-one, **BW-CP-139**

75%MeOH+0.1%HCOOH, 100uL/min,

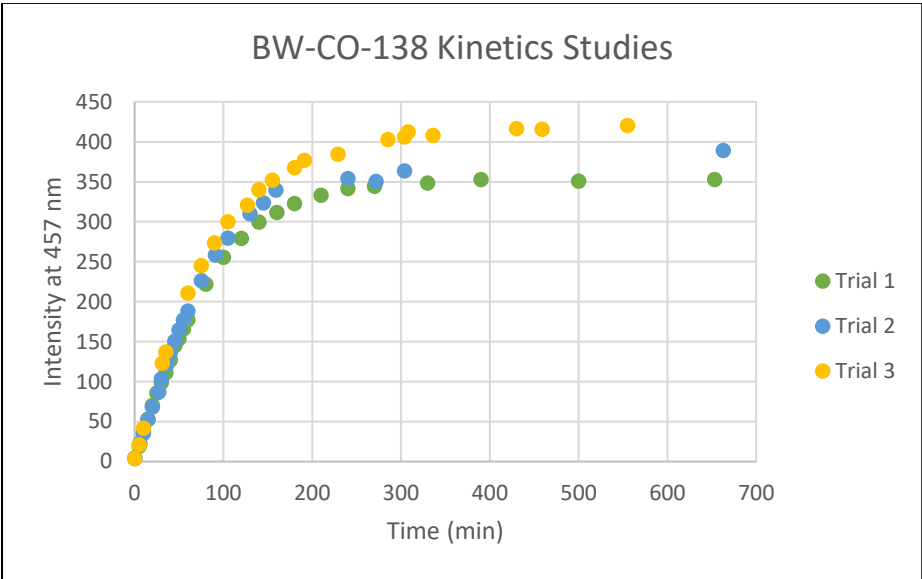
David_BW_CP_140_ESI_pos_BWang_02232022 301 (1.664) Cm (257:301-119:227)

1: TOF MS ES+
6.66e7

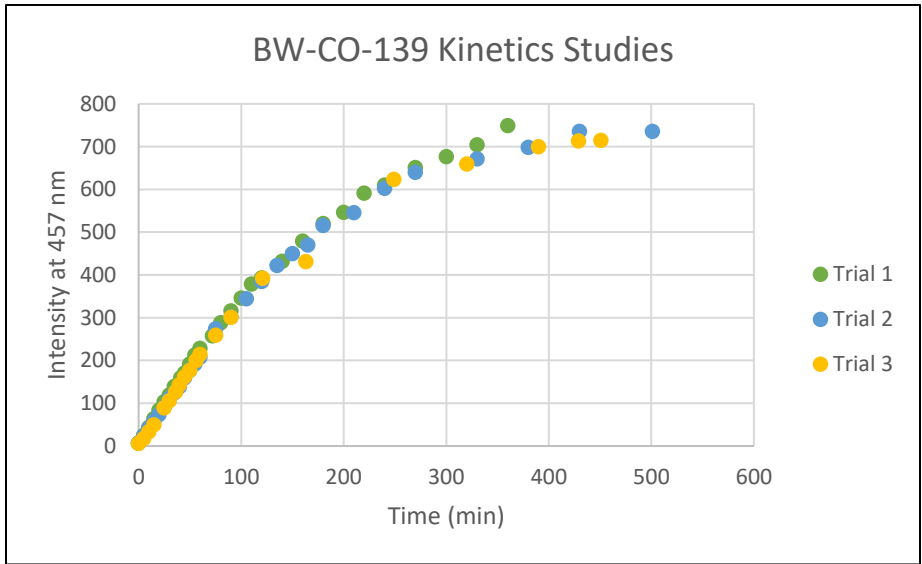


Mass Spectrum of **4c**, 2-isopropyl-6-(4-methoxyphenyl)-3,4-dihydroacenaphtho[1,2-h]isoquinolin-1(2H)-one, **BW-CP-140**

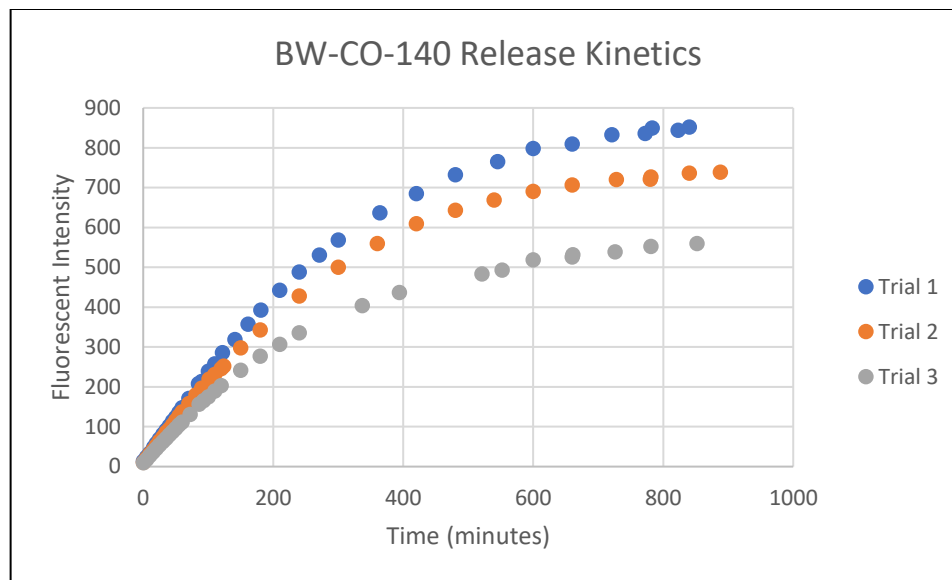
Fluorescence Spectra



Kinetic studies of **BW-CO-138**.



Kinetic studies of **BW-CO-139**.



Kinetic studies of **BW-CO-140**.